A Basic Study on Solid-liquid Interfacial Reactions of Heavy Metal Ions in Soil Systems

Akane MIYAZAKI

PhD Thesis

A Basic Study on Solid–liquid Interfacial Reactions of Heavy Metal Ions in Soil Systems

Akane MIYAZAKI

Multi–Disciplinary Studies
Graduate School of Art and Sciences
The University of Tokyo

CONTENTS

CHAPTER 1: INTRODUCTION

1-1 PURPOSE AND SIGNIFICANCE OF THIS STUDY

Soil is one of the bases of our life. In soil systems, a great variety of substances are constantly circulating, the elements essential to plant growth, for example, and it is this movement of elements that makes soil irreplaceable. However, our knowledge about the behavior of elements in soil systems is quite limited. This is due to two factors: the complex composition of soils, and the fact that the chemical reactions on the surface of soil particles are not well understood.

Today, one of the most serious environmental problems is pollution of the soil by heavy metals. Human activity adds heavy metals to soil systems either by direct means or indirectly through the air or water. Such heavy metals move about in soil systems, repeatedly undergoing the processes of dissolution, transportation and accumulation. These movements are controlled by solid-liquid interfacial reactions between the surface of soil particles and the heavy metals in soil water. Therefore, when we deal with soil pollution by heavy metals, it is essential to understand how heavy metals behave at the solid-liquid interface.

The purpose of this study is to describe the solid-liquid interfacial reactions of heavy metals in soil systems as chemical reactions, and to know what occurs at the solid-liquid interface. For this purpose, I adopted amorphous aluminosilicate as a model substance to represent the surface of soil particles, because I thought a model substance would be necessary to deal with the general features of something as complex as soil systems.

This study could be helpful in preventing and dealing with environmental problems affecting soil such as pollution by heavy metals and the effects of acid rain. It may also prove useful in geochemistry's attempt to understand the circulation of heavy metals in nature and their impact on human society. Moreover, this study may contribute to any field of chemistry related to solid-liquid interfacial reactions.

1-2 CHARACTERISTICS OF THIS STUDY

This study has two main characteristics.

The solid-liquid interfacial reaction between soil particles and heavy metal ions is known as "adsorption phenomena". Extremely high affinity of heavy metal ions to clay minerals is called "specific adsorption". These terms are qualitative and their mechanism has not been made clear.

In this study, I divided the content of so-called adsorption phenomena in soil systems into the following three reactions, depending on their respective mechanisms:

(1) *Precipitation on the solid surface*. This contains no chemical reaction between the solutes and the solid surface. The solid plays only the role of the nucleus for precipitation.

(2) *Outer-sphere complex formation*. Ions with a charge opposite to the solid surface are attracted to the charged surface by electrostatic force. The mechanism of this reaction is ion exchange. Therefore, their affinity to the surface is decided by the radii and charge of the ions. In the complex formed there is no direct bond between the surface groups of the solid and the metal ions, and there are hydrating H_2O molecules between them.

(3) *Inner-sphere complex formation*. This is so-called specific adsorption. Ions make bonds with the surface groups of the solid. The affinity to the solid surface can be represented by the values of equilibrium constants.

Using the above categories, I deal with adsorption phenomena quantitatively as chemical reactions. This is the first main characteristic of this study.

In this study, the soil system is assumed to consist of three phases: solid,

liquid and gas. This is the second main characteristic of this study. The gas phase of soil systems is called soil air, although its composition is quite different from that of the atmosphere. For example, the partial pressure of CO_2 in soil air is reported to be 10 to 100 times greater than that of the atmosphere. Because CO_2 gas dissolves in water, the partial pressure of CO_2 can affect the composition of the co-existing liquid phase. However, solid-liquid interfacial reactions in soil systems have hitherto been discussed generally as consisting of only the solid and liquid phases. In this study, I have taken soil gas into consideration as an important factor which could affect solid-liquid interfacial reactions.

1-3 OUTLINE OF THIS WORK

This thesis is composed of six chapters. The content of each chapter is as follows.

In Chapter 1, the purpose and outline of this work are described. The characteristics which distinguish it from previous works are also discussed.

In Chapter 2, I state the reason why I adopted amorphous aluminosilicate as the model substance for the surface of soil particles. Then the preparation of synthetic amorphous aluminosilicate and its characteristics are described. I

discuss the chemical properties of the amorphous aluminosilicate used in this study.

Chapter 3 describes the solid–liquid interfacial reactions between zinc ions and the surface of the synthesized amorphous aluminosilicate. Firstly, I explain the newly developed method to conduct batch adsorption experiments for this study. Secondly, using this experimental method, I have discussed quantitatively the mechanisms of the solid–liquid interfacial reactions of zinc ions on the surface of aluminosilicate. Then several contributions of the aluminol groups and silanol groups to the solid–liquid interfacial reactions are discussed. Because most natural soil particles are complex oxides like aluminosilicate, which is a complex oxide of aluminum and silicon, I suggest how we might deal with solid–liquid interfacial reactions on such complex oxides.

In Chapter 4, the chemical states of heavy metals at the solid surface are discussed in regard to ferric and ferrous ions, as well as zinc ions. There are few analytical methods which are effective in determining the chemical states of heavy metals at solid–liquid interfaces. In this study, Mössbauer spectroscopy and the XAFS (X–ray Absorption Fine Structure) method are adopted to observe the chemical states of heavy metal ions on the wet surface of amorphous

aluminosilicate. The solid–liquid interfacial reactions of these heavy metals are discussed with reference to data from the adsorption experiment described in Chapter 3.

In Chapter 5, the effect of co–existing chemical species on solid–liquid interfacial reactions is discussed. More specifically, the effect of the concentration of hydrocarbonate ions on solid–liquid interfacial reactions between zinc ions and amorphous aluminosilicate is discussed. The concentration of hydrocarbonate ions depends on the partial pressure of CO_2 in soil air. Therefore, this is an examination of whether the composition of soil air can affect the solid–liquid interfacial reaction in soil systems.

Finally, in Chapter 6 the conclusion of this study is presented along with discussion of the future prospects for research along these lines.

CHAPTER 2: AMORPHOUS ALUMINOSILICATE AS A MODEL SUBSTANCE FOR THE SURFACE OF SOIL PARTICLES

2-1 INTRODUCTION

The solid phase of soil can be divided into four components: coarse and colloidal particles of inorganic substances, organic substances, and living organisms (Ichikuni 1989). Two of them are generally recognized as the main components which contribute to adsorption phenomena in soil systems: colloidal inorganic substances such as clay minerals and hydrated oxides, and organic substances like humin. However, there is still uncertainty regarding the relative extent to which these substance contribute to heavy metal movement in soil systems.

In this study, I adopted amorphous aluminosilicate as a model substance for the surface of soil particles by the following ideas. Firstly, I excluded organic substances from possible model substances, because they include a great variety of compositions and structures, and there is no general theory about adsorption sites. Additionally, organic substances rarely exists by themselves in soil, and usually they form a complex with clay minerals (Yoshida 1985). Secondly, I selected aluminosilicate among colloidal inorganic substances,

because it is the most abundant substance in soil systems and also known to adsorb heavy metal ions quite specifically. Thirdly, I particularly chose to adopt *amorphous* aluminosilicate as a model substance, because amorphous aluminosilicate is known to deeply affect heavy metal movements in soil systems (Yamamoto 1982). Amorphous aluminosilicate shows extremely high affinity to heavy metal ions. For example, the value of cation exchange equilibria between Ca^{2+} and heavy metal ions ranges from 1000 to 100,000 for amorphous aluminosilicate (Wada 1980), while the value is 0.8 to 6.1 for crystalline clay minerals (Bruggenwert and Kamphorest 1979). Among soil particles, amorphous aluminosilicate is known to have the greatest affinity to heavy metal ions (Saegusa 1989). Moreover, amorphous aluminosilicate exists extensively on the surface of soil particles. Amorphous silica-alumina layers are reported to exit on the surface and the edge of most crystalline minerals (Yariv and Cross 1981).

In soils, the most typical amorphous aluminosilicate is allophane, which is represented by the general formula $1\sim2SiO_2 \cdot Al_2O_3 \cdot nH_2O$. Allophane is defined as "the name of a group of clay-size minerals with short-range order which contain silica, alumina and water in chemical combination" (Parfitt 1990). Allophane is the main clay mineral in Andisol, which is the most important agricultural soil in Japan. Many peculiarities of Andisol have been thought to be

due to Allophane (Shoji 1985).

From the above, I concluded that amorphous aluminosilicate, such as allophane, is a suitable model substance for the surface of soil particles when we deal with heavy metal movement in soil systems. In this study, the co-precipitation method was used to obtain an allophane-like amorphous aluminosilicate. In the following sections, the synthesis method and the characteristics of the substance obtained are described.

2-2 EXPERIMENTAL

(1) Synthesis of Amorphous Aluminosilicate

Aluminosilicate was prepared in reference to coprecipitation method described by Ossaka *et al.*(1971). SiO_2 was melted together with NaOH in a nickel pot so as to obtain sodium silicate. A mixed solution of sodium silicate and aluminum sulfate was prepared at pH 2 by adding H_2SO_4. In the mixed solution, the concentrations of Si and Al were both adjusted to 1 mmol / L. Then the pH value of the mixed solution was increased by a hexamethlenetetramine solution to obtain coprecipitate. After boiling and filtration, the coprecipitate was washed and dried in the air for two weeks. The air-dried coprecipitate was ground to a powder in an agate mortar and preserved in a styrol bottle.

(2) Characterization of Synthesized Aluminosilicate

The co-precipitate obtained were characterized by X-ray powder diffraction pattern (XRD), differential thermal analysis, and thermo-gravimetry (DTA-TG) curve. The water content, Al:Si molar ratio and value of pH_{ZPC} (pH of zero point of charge) were also determined.

XRD patterns were obtained using a Rigaku Geiger-flux RAD-IIA with Cu-Kα radiation (30kV, 20mA), and scanning from 10-70° 2θ. DTA-TG

curves were obtained using Rigaku DTA–TG PTC–10A, with increasing rate of temperature, 20deg / min from 20 to 1000°C. The concentration of Al and Si were measured by atomic absorption spectrophotometry, using the method of standard addition. The water content was measured by ignition loss at 1000°C.

The point of pH where the surface charge caused by binding of H^+ or OH^- is equal to zero is called the pH *of zero point of charge*, pH_{ZPC} (Stumm and Morgan 1981). In this study, values of pH_{ZPC} were obtained by following method. Aquatic solutions of 0.1N $NaNO_3$ were adjusted to various pH by using an aquatic solution of NaOH or HNO_3. The co–precipitate obtained was added to the solution and the resultant suspension, of which concentration was 1 g / L, was stirred by a magnetic stirrer. After two hours of stirring, pH values of the suspensions were measured. If the original solution has the same pH value as pH_{ZPC} of the solid, pH of the original solution should not be changed by adding the coprecipitate. Thus the value of pH_{ZPC} was obtained as the pH value of original solution, of which pH was not changed by adding the co–precipitate obtained.

2–3 RESULTS AND DISCUSSION

The co–precipitate obtained was a white gel. After being air–dried, it became a light white solid which was easily ground to a powder.

The XRD pattern of the co–precipitate obtained is shown in Fig. 2–1. In the XRD pattern, there are no clear and sharp peaks, but only a broad peak, which is peculiar to the amorphous substances seen around $2\theta = 27°$. Cruz and Real (1991) measured XRD patterns of natural allophanes from Gibraltar in Spain, and reported that the diffractgram of natural allophane showed a maximum between 3.42 and 3.30Å. These values correspond respectively to 26.04° and 27.00° in Fig. 2–1. Therefore, the diffractgram shown in Fig. 2–1 can be said to be same as the diffractgram of natural allophane.

The DTA and TG curves of the co–precipitate obtained are shown in Fig. 2–2. The DTA curve has an exothermic peak around 980°C. This peak is typical of aluminosilicate (Yokoyama 1982). Since both Al_2O_3 and SiO_2 don't show the exothermic peak by themselves (Ossaka 1962), the co–precipitate is not a mere mixture of Al_2O_3 and SiO_2 but an aluminosilicate. The DTA curve in Fig. 2–2 has an endothermic peak at about 100 to 300°C, too. This pattern is quite similar to the general shape of allophane's DTA curves (Ossaka 1962,

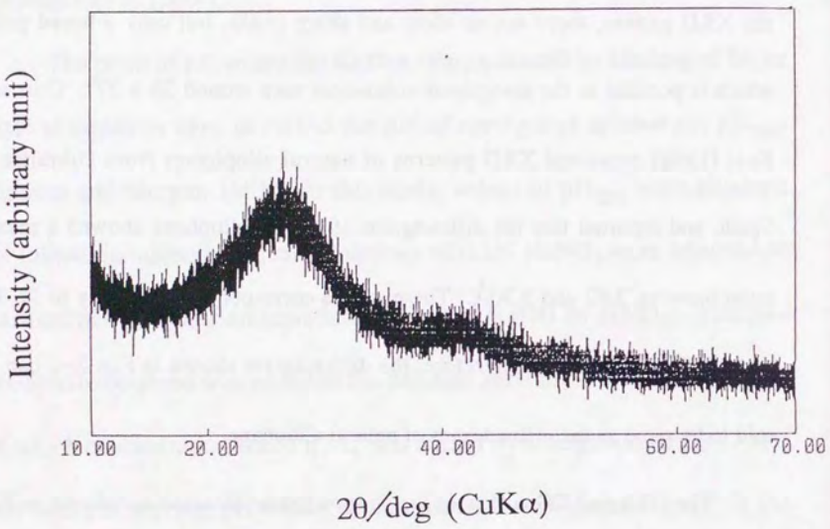

Figure 2–1 The XRD pattern of the co–precipitate obtained.

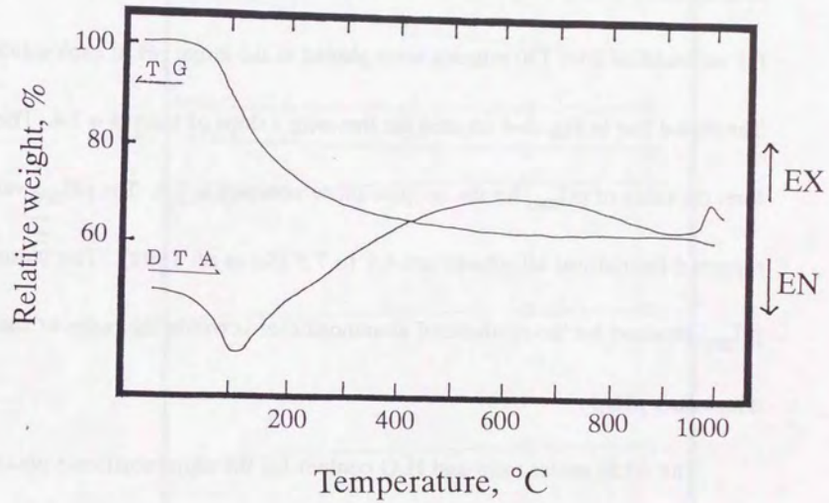

Figure 2–2 The DTA and TG curves of the co–precipitate obtained.

Aomine 1958).

Figure 2–3 shows temporal changes in pH values of suspensions after the co–precipitate was added to $NaNO_3$ solutions. Figure 2–3 indicates that the suspensions reached a equilibrium after 120 min. In Fig. 2–4, the pH values of the suspensions after 120 minutes were plotted to the initial pH of each solution. The dotted line in Fig. 2–4 crossed the line with a slope of 1 at pH = 7.4. Therefore, the value of pH_{ZPC} for the co–precipitate obtained is 7.4. The pH_{ZPC} values reported for natural allophane are 4.1 to 7.9 (Su *et al.* 1992). The value of pH_{ZPC} obtained for the synthesized aluminosilicate is within the range of natural allophane's pH_{ZPC}.

The Al:Si molar ratio and H_2O content for the aluminosilicate obtained are summarized in Table 2–1. The co–precipitate obtained almost maintains the Al:Si molar ratio of the original solution. The value of water content for the co–precipitate, 42.2%, is within the range of the reported H_2O content of natural allophane, 33 to 44% (Aomine 1958).

From the above measurements, the precipitate obtained would seem to be characterizable as allophane. However, there is a controversy about the defini–

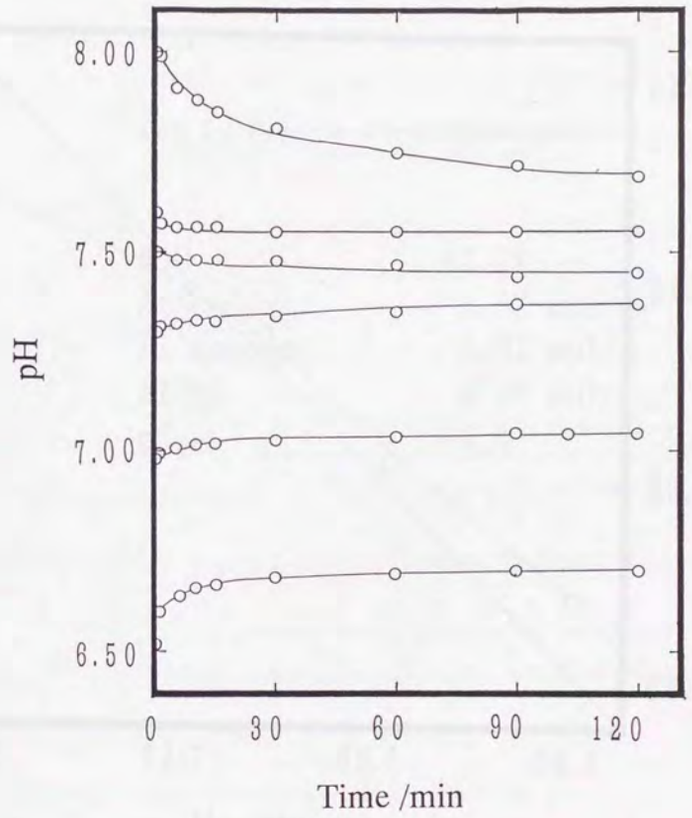

Figure 2–3 Temporal changes in pH values of suspensions after the addition of the co–precipitate. The pH values at 0 minute mean the pH value of original 0.1 *N* $NaNO_3$ solution.

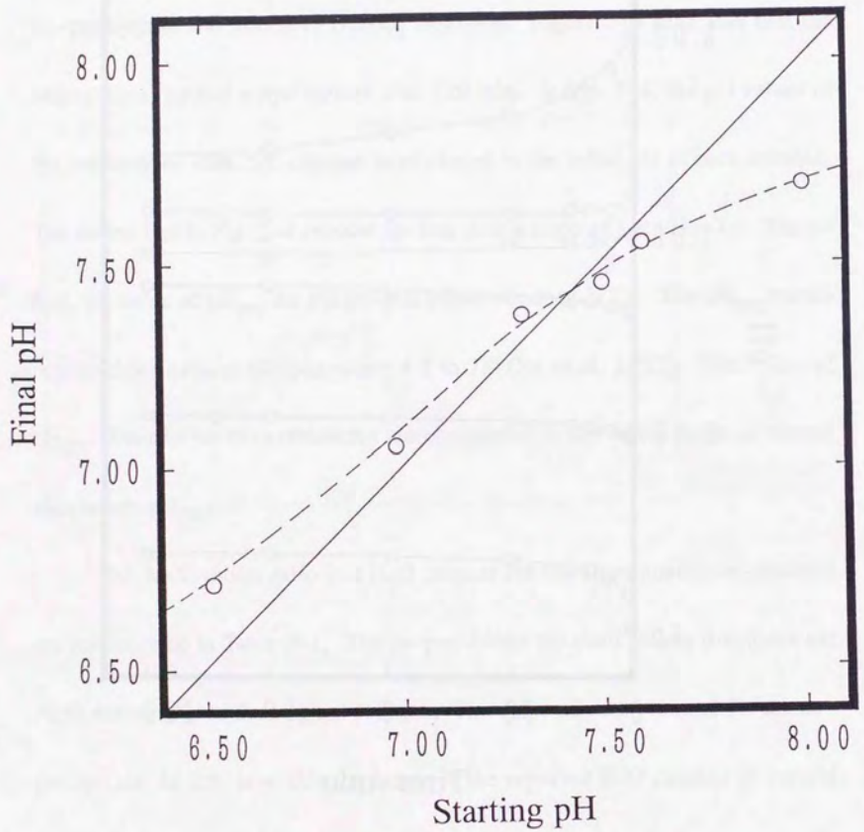

Figure 2–4 Rerationship between the pH values of original solution and equilibrated suspension after 120 minutes from the addition of the co–precipitate.

Table 2–1 Properties of co–precipitate obtained.

H_2O	42.2%
Al content	5.52 mol/g
Si content	5.91 mol/g
Al/Si	0.93 mol/mol
pH_{ZPC}	7.4

tion of allophane from a morphological point of view (Huang 1991). For example, Wada (1989) limited the term allophane to hydrous aluminosilicate with a hollow spherical morphology. Since the morphology of the co-precipitate obtained was not determined in this study, the substance obtained should be characterized as allophane-like amorphous aluminosilicate.

2-4 CONCLUSION

The substance obtained by co-precipitation was characterized as allophane-like amorphous aluminosilicate with an Al:Si molar ratio of about 1. This substance is suitable as a model for the surface of soil particles. In the following chapters, solid-liquid interfacial reaction is discussed using the synthesized amorphous aluminosilicate as the solid phase.

REFERENCES

Aomine, S (1958) Allophane in Soils. *Nihon-Dojyou-hiryougaku-zassi*. **28**, 40-516.

Bruggenwert, M.G.M. and Kamphorst, A. (1979) Survey of Experimental Information on Cation Exchange in Soil Systems, in *Soil Chemistry*, B.Phsyco-chemical Model. (ed.) G.H.Bolt, Elsevier, Amsterdam pp.141-203.

Cruz, M.D.R and Real,M.N. (1991) Practical determination of allophane and synthetic alumina and iron oxide gels by X-ray diffraction. *Clay Minerals*, 26, 377-387.

Huang, P.M. (1991) Ionic factors affecting the formation of short-range ordered aluminosilicates. *Soil Sci. Soc. Am. J.*, **55**, 1172-1180.

Ichikuni, M. (1989) 1 Introduction in *Soil Chemistry*, (ed.) *Nihon-kagakukai*, Gakujyutu-syuppann-center, Tokyo, pp.2-5.

Ossaka, J. (1962) Thermal changes of hydrated SiO_2-Al_2O_3 clay minerals. *Adv. Clay Sci.*, 4, 33-47.

Ossaka, J. et al. (1971) Coexistence state of synthesized iron bearing alophane (Al_2O_3-SiO_2-Fe_2O_3-H_2O system). *Bull. Chem. Soc. Jpn.*, **55**, 975-978.

Parfitt, R.L. (1990) Allophane in New Zealand. *Aust. J. Soil. Res*, **28**, 343-60.

Saegusa, M. (1989) 5. Clay minerals in *soil science*, (ed.) *Nihon-kagakukai*, Gakujyutu-syuppann-center, Tokyo, pp.50-65.

Shoji, S. (1985) *Kagaku to Seibutu* **22**, 242–250.

Stumm, W. and Morgan, J.J. (1981) 10. The solid–solution interface. in *Aquatic Chemistry* 2nd Ed. Wiley interscience publication, New York, pp.599–684.

Wada, K. (1980) Mineralogical Characteristics of Andisols in Soils with Variable Charge. *New Zealand Soc. Soil Science*, (ed.) B.K.G. Theng, pp.87–107.

Wada, K. (1989) Allophane and imogorite in *Minerals in soil environment* 2nd Ed. (ed.) J.B.Dixon and S.B. Weed, SSSA, Madison, WI., pp.1051–1087.

Yamamoto, K. (1982) Roles of amorphous clay minerals in heavy metal adsorption phenomena. *Nihon–Dojyougaku–Zassi*, **53**, 355–366.

Yariv, S. and Cross, C. (1981) *Geochemistry of Colloid System*.

Yokoyama, T. (1982) Polymerization of silicic acid adsorbed on aluminum hydroxide. *Bull. Chem. Soc. Jpn.*, **55**, 975–978.

Yoshida, M. (1985) 2. Absorption ability and nature of soil organic substances. in *Adsorption phenomena in soil–bases and application*, (ed.) Nihon–dojyo–hiryou–gakkai, Hokuyuusya, Tokyo, pp.59–84.

CHAPTER 3: SOLID–LIQUID INTERFACIAL REACTIONS BETWEEN ZINC IONS AND AMORPHOUS ALUMINOSILICATE

3–1 INTRODUCTION

The adsorption phenomena of ions to soil particles have been explained by mainly three models (Okazaki and Yamane 1983): surface complex formation model (ligands model), hydrolysis model (ion–solvent interaction model), and crystal field model. In these days, the surface complex formation model seems to be the most general and widely accepted model among them.

Surface complex formation models are chemical models that use an equilibrium approach to describe the formation of complexes at the oxide–solution interface (Goldberg 1991). Unlike empirical models, such as the Langmuir and Freundlich adsorption isotherm equations, chemical models explicitly define surface species, chemical reactions, equilibrium constant expressions, and surface activity coefficient expressions. Additional advantages of surface complex formation models are inclusion of mass and charge balance equations, and consideration of the charge on both adsorbate and the adsorbent.

To provide a molecular description of adsorption processes, surface complex formation models assume a detailed structure of the interfacial region. Surface species are defined as outer–sphere complexes, containing at least one water molecule between the adsorbate ion and the surface functional group, or

as inner-sphere complexes, containing no water molecules between the adsorbate ion and the surface functional group.

Amorphous aluminosilicates are assumed to have such surfaces as shown in Fig. 3-1. There are two kinds of charges on the surface. One is variable surface charges, caused by the ionization of weakly acidic surface -OH groups which respond to changes in pH and ionic strength. The other is permanent surface charges, caused by ionic substitution of lattice structure (Anderson and Sposite 1991). These two surface charges severally cause to form different surface complexes (Evans 1989). At the permanent surface charge site, hydrated cations are attracted by electrostatic force and form outer-sphere complex. The mechanism of this reaction is an ion exchange. Therefore, the ion with the higher charge is more preferred by the adsorbent, and for ions of the same valance, the metal with the higher atomic number is preferred (Dorfer 1972). On the other hand, at the variable surface charge site, ion reacts with surface -OH groups directly and form inner-sphere complex. The mechanism of this reaction is a ligand exchange. Therefore, the extent of adsorption depends on the intrinsic formation constants for the complexation reactions.

The specific or selective adsorption commonly refers preferential adsorption of heavy metals present at very low concentration relative to macro amount of a competing cation (Ziper *et al.* 1988). This phenomena have been expected

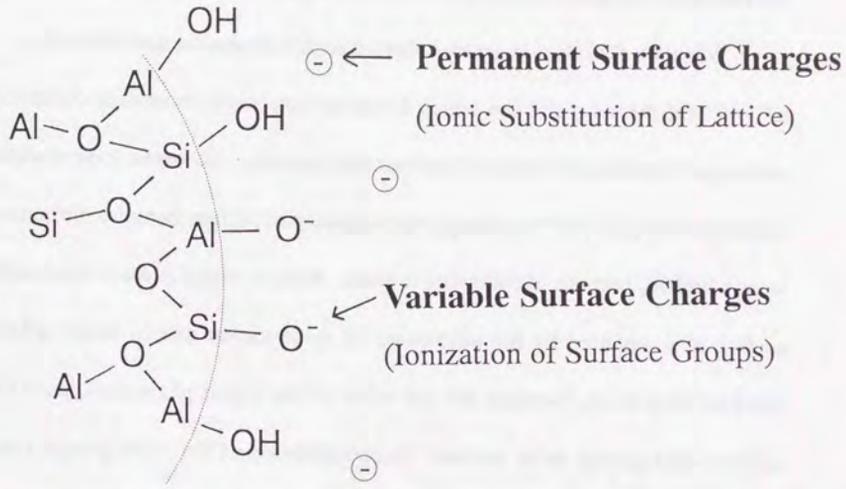

Figure 3-1. The surface of amorphous aluminosilicate.

to be inner–sphere complex formations whose intrinsic formation constants are larger than those of competing cations. However, it has not been accomplished yet to describe the inner–sphere complex formation quantitatively, because there is a difficulty due to the nature of the surfaces of oxides suspended in solution.

When we deal with an inner–sphere complex formation quantitatively, H^+ / M^{n+} (M means metal ion which forms an inner–sphere surface complex) exchange stoichiometry is one of the essential quantity. However, experimental data concerning H^+ / M^{n+} exchange stoichiometry of surface complex formation is very limited, because of following reasons. Protons which released from solid surface accompanied by the adsorption of some cation due to inner–sphere complex formation, decrease the pH value of the liquid phase and cause the surface –OH groups to be ionized. Such ionization of the –OH groups consumes the H^+ and makes it difficult to know the amount of H^+ released by the inner–sphere complex formation itself.

The purpose of this chapter is to describe quantitatively the solid–liquid interfacial reactions between amorphous aluminosilicate and zinc ions using surface complex formation models. For this purpose, I construct a new experimental method which makes possible to obtain proton exchange stoichiometry. Then, using the new method I describe solid–liquid interfacial reaction quantitatively. Here zinc has been adopted, because it is one of the most abundant heavy metal in natural water (Runnels et al. 1992). Moreover, it is essential for

animals and higher plants; at the same time, excess amount of Zn have been reported to be harmful (Kiekens 1990).

3–2 Experimental

(1) A new batch method

A constant pH method for a batch adsorption experiment was developed. This is a kind of potentiometry in which the pH value and ionic strength of the reacting suspension are kept strictly constant. Therefore, it is unnecessary to consider the change of variable charge site density. The H^+ ion released by the solid phase is immediately neutralized by an alkaline solution, and the amount of alkaline solution suggests the amount of H^+ released by surface–complexation. The details of this method are described below.

Stock suspension of synthetic aluminosilicate and stock solution of $Zn(NO_3)_2$ and $NaNO_3$ were prepared at pH 6.50 and ionic strength 0.1, before the batch adsorption experiment. The values of pH and ionic strength were adopted based on the fact that the pH value and the ionic strength of natural water are generally ranging from 4.5 to 7 and within 0.02 0.14, respectively. By mixing these solutions, it becomes possible to keep constant ionic strength and pH value and constant concentration of aluminosilicate in the reacting suspension.

The 0.4 g synthesized and air–dried amorphous aluminosilicate was suspended in 200 ml of 0.1 *N* $NaNO_3$ solution to get 2 g / L mother suspension. This suspension has been stirred by a magnetic stirrer through the experimental period. Liquid paraffin was used to cover the suspension and to prevent dissolution of CO_2 from air into the suspension. The effect of liquid paraffin is shown in Fig. 3–2. The pH of this suspension was monitored by pH electrodes, and 0.01 *N* NaOH was added by an automatic titrator (METROHM 614 Impulsomat, Dosimat E 535) to maintain the pH at 6.50. Figure 3–2 shows that covering with liquid paraffin shortened the time to reach equilibrium. The 0.01 *N* NaOH solution contained 0.09 *N* $NaNO_3$; thus its ionic strength was also 0.1. These pH adjustments continued for a day at 25 $\pm$ 0.1 °C.

The stock solution of Zn^{2+} was prepared by dissolving $Zn(NO_3)_2$ salt. Both the Zn^{2+} stock solution and 0.1 *N* $NaNO_3$ solution were covered with liquid paraffin and had been maintained at pH 6.50 in a similar manner to the conditioning of the aluminosilicate suspension.

The adsorption experiment was started by mixing 50 ml of the 2g / L aluminosilicate stock solution and 50 ml of 0.1 *N* $NaNO_3$. The resulting 1g / L aluminosilicate suspension was covered with liquid paraffin and had been stirred by a magnetic stirrer. The pH of this suspension had been maintained at 6.50 by adding 0.01 *N* NaOH with an automatic titrator. After 30 minutes, 5 ml of this suspension was taken out and filtered rapidly to confirm the initial experimental condition. Zinc concentration of the filtrate was measured by atomic absorption spectroscopy, making sure the background was not detected.

Then, X ml of Zn^{2+} ion stock solution was added into the reacting sus–

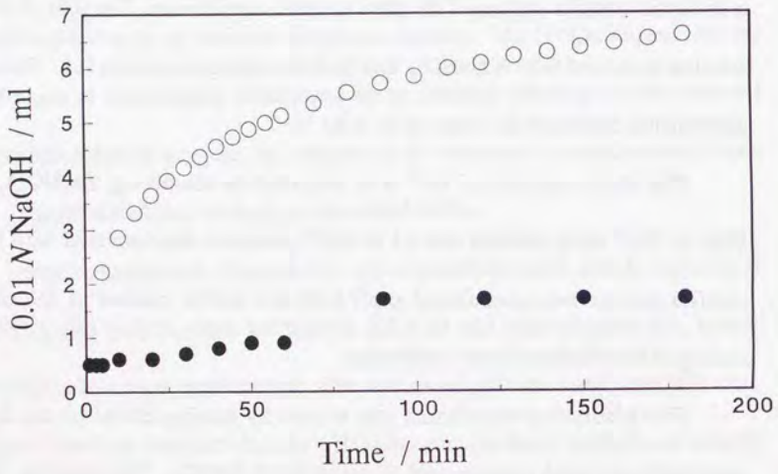

Figure 3–2. Temporal changes of the amount of 0.01 *N* NaOH consumed to adjust the pH of the suspension of amorphous aluminosilicate at 6.50. The preconditioning of the suspension was compared under the existence of liquid paraffin (●) with the absence of it (○).

pension. At the same time, X ml of aluminosilicate stock solution was added. In this way the ionic strength and the concentration of aluminosilicate remained constant. For 30 minutes, the 0.01 *N* NaOH solution was added to maintain the pH of the reacting suspension at 6.50. Then 5 ml of the suspension was taken out and filtered to measure Zn concentration in the liquid phase.

The same procedure were repeated to increase the Zn^{2+} concentration. In the reacting suspension, ionic strength remained constant at 0.1 and the concentration of aluminosilicate was kept at 1 g / L. Only the concentration of Zn^{2+} was increased step by step.

At every step, the total concentration of Zn^{2+} can be calculated. The concentration of Zn^{2+} in the liquid phase of the reacting suspension was obtained by atomic absorption spectroscopy. The amount of H^+ released from the solid phase was obtained from the amount of 0.01 *N* NaOH added to neutralize the H^+ and to maintain constant pH by an automatic titrator.

(2) Zn adsorption on amorphous aluminosilicate with Al/Si = 1

Solid–liquid interfacial reactions between the synthesized amorphous aluminosilicate and Zn ions were analyzed using the batch adsorption method developed in 3–3 (1). In the experiments, solid concentration were maintained at 1g / L, and 10 mmol / L Zn^{2+} stock solution was used.

Another experiment was also performed using a similar procedure to

check the results obtained by the above experiment. In this case, the total concentration of Zn in the reacting suspension was maintained at 0.5 mmol / L and only the total volume of the suspension was increased.

(3) Zn adsorption in a lower concentration of amorphous aluminosilicate

The solid-liquid interfacial reactions between Zn ions and the synthesized amorphous aluminosilicate were studied in low concentration of solid. The concentration of the solid was maintained at 0.1 g / L. For this experiment, 25 mmol / L of $Zn(NO_3)_2$ solution was added to the reacting suspensions.

(4) Zn adsorption onto aluminosilicate with different Al / Si ratios

Aluminosilicates with different Al / Si ratios and Al_2O_3 were synthesized and the batch adsorption experiment developed in 3-3 (1) was performed using these solids. The aluminosilicates with different Al / Si ratio were synthesized by the same procedure as the co-precipitation method described in Chapter 2, but the co-precipitates obtained for this experiment were washed more intensively until conductance of their washing water became lower than 10 μS / cm. In the original solution, the Al / Si molar ratio was adjusted 0.5, 1, and 2, and the concentration of Al + Si were 2 mmol / L for all samples. A precipitation of Al_2O_3 was also obtained by the similar method. A SiO_2 gel (Merck, Silica gel

60) was used for comparison. In the adsorption experiments using these solids, the concentration of $Zn(NO_3)_2$ aquatic solution, which was added to the reacting suspension, was basically 10 mmol / L.

3–3 RESULTS AND DISCUSSION

(1) Surface Complex Formation Between Zn Ions and Amorphous Aluminosilicate

The newly developed batch method enabled to maintain the pH value and ionic strength constant at 6.50 and 0.1, respectively. In the reacting suspension only the concentration of Zn^{2+} was varied: the concentration of total Zn^{2+} was increased from 0 to 2 mmol / L step by step. After the addition of the Zn^{2+} stock solution, the pH value of the reacting suspension was readjusted to 6.50 for 30 minutes. Figure 3–3 shows the temporal variation of the amount of 0.01 *N* NaOH solution added to the suspension to readjust its pH value. It is clear that H^+ is released to the liquid phase, because the alkaline solution was added, though the pH values of both the reacting suspension and added Zn^{2+} stock solution were already maintained at 6.50 before mixing. Figure 3–3 shows that the addition of alkaline solution is basically completed within 5 minutes, namely the H^+ releasing reaction and following neutralization reached equilibria within 30 minutes after the addition of Zn^{2+} stock solution. Therefore, one may surmise that the reacting time, 30 minutes, is enough to obtain equilibrium state.

Figure 3–4 shows the relationship between the concentration of total Zn^{2+} in the reacting suspension and the amount of Zn^{2+} retained by 1 g of the amorphous aluminosilicate. The observed data follow a straight line in Fig. 3–4. This fact shows that the solid–liquid interfacial reaction which took place in the

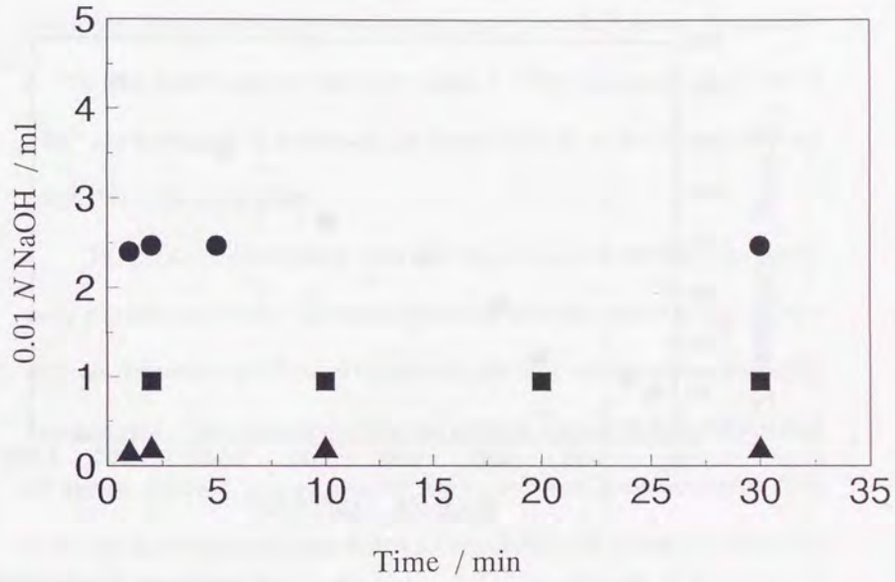

Figure 3-4. The amount of Zn^{2+} retained by 1 g of amorphous aluminosilicate at each concentration of total Zn^{2+} in the reacting suspension.

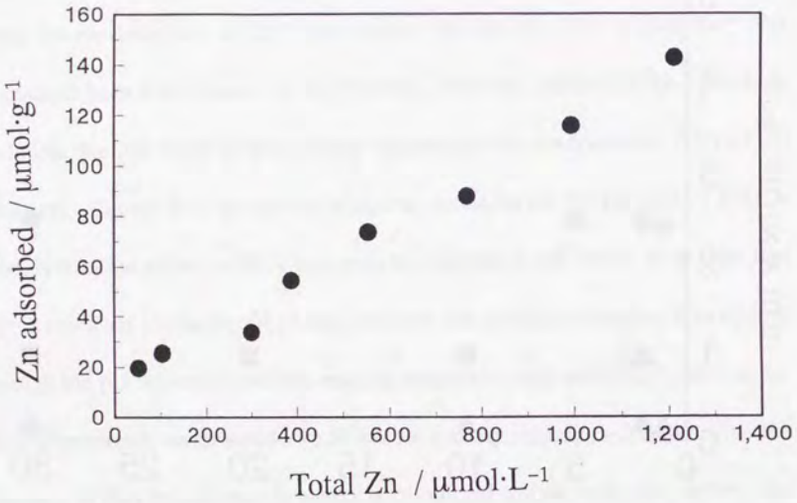

Figure 3–4. The amount of Zn^{2+} retained by 1 g of amorphous aluminosilicate at each concentration of total Zn^{2+} in the reacting suspension.

reacting suspension had a single mechanism in all the range of total Zn^{2+} concentration studied.

Figure 3–5 shows the relationship between absolute amount of retained Zn^{2+} and released H^+. The each point in Fig. 3–5 represents the data at every step of the process, increasing the concentration of total Zn^{2+} from 0 to 2 mmol / L. The data follow a straight line with a slope 2. This relationship shows that if a Zn^{2+} ion is retained by the amorphous aluminosilicate, at that time two H^+ are released into the liquid phase.

To check the relationship shown in Fig. 3–5, I did another experiment using a similar procedure. The concentration of total Zn in the reacting suspension was maintained at 0.5 mmol / L and only the total volume of the suspension was increased. The result showed that the absolute amount of both the released H^+ and the adsorbed Zn^{2+} were varied step by step with good correlation (Fig. 3–6), and the experimental data follow a straight line with a slope 2. It is clear that a Zn^{2+} adsorption onto the amorphous aluminosilicate is accompanied by two H^+ release.

These data can be explained by a surface complex formation model; an inner sphere complex formation between a Zn^{2+} ion and two –OH groups, aluminol or silanol groups, on the surface of the amorphous aluminosilicate. When a heavy metal ion M^{n+} comes to the surface of aluminosilicate, aluminol

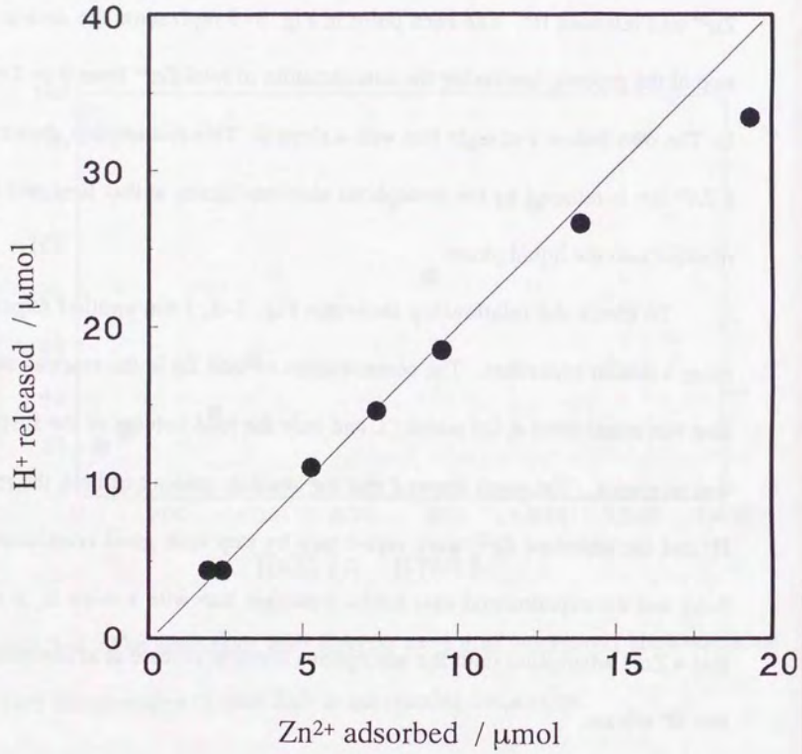

Figure 3–5. Relationship between the absolute amount of adsorbed Zn^{2+} and the absolute amount of released H^+. The total concentration of Zn^{2+} was varied from 0 to 1.2 mmol / L.

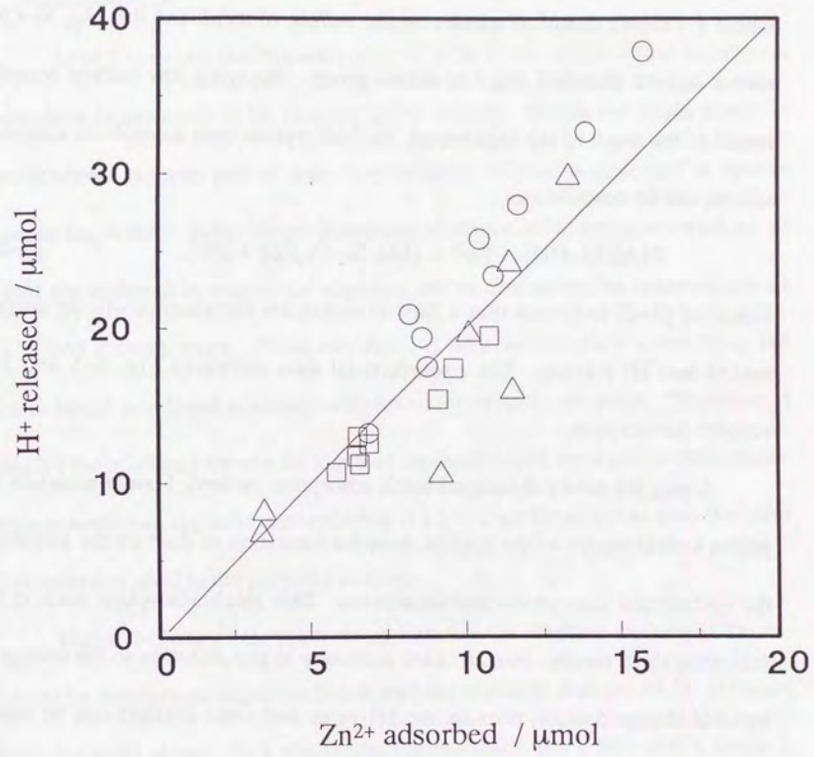

Figure 3–6. Relationship between the absolute amount of adsorbed Zn^{2+} and the absolute amount of released H^+. Total volume of the suspension was increased, and the total concentration of Zn^{2+} was kept constant at 0.5 mmol / L.

or silanol groups coodinate to the ion with releasing H^+, and form a surface complex. It can be describe as

$$n\{\text{Al, Si} - \text{OH}\} + M^{n+} = \{(\text{Al, Si} - \text{O})_n M\} + nH^+, \qquad [3\text{–}1]$$

where { } shows chemical species on the surface of solid, and the {Al, Si–OH} means surface aluminol and / or silanol group. Applying this surface complex model to the result of the experiment, Zn^{2+} adsorption onto amorphous alumino–silicate can be described as

$$2\{\text{Al, Si–OH}\} + Zn^{2+} = \{(\text{Al, Si–O})_2\text{Zn}\} + 2H^+. \qquad [3\text{–}2]$$

Equation [3–2] indicates that a Zn^{2+} retention on the aluminosilicate surface makes two H^+ release. The experimental data shown in Fig. 3–5 and 3–6 support this reaction.

Using the newly developed batch adsorption method, I could ascertain the proton stoichiometry of the surface complex formation of Zn^{2+} on the surface of the synthesized amorphous aluminosilicate. This batch adsorption method has following three merits. First, it is not necessary to pay attention to the change of variable charge density, because the pH value and ionic strength can be main–tained constant. Second, it is possible to determine accurately the amount of H^+ released from the solid phase to the liquid phase. Third, in this adsorption experiment we can vary the total concentration of metal ions in a reacting sus–pension step by step. This batch adsorption method was found to be effective to deal with solid–liquid interfacial reactions quantitatively.

(2) Surface Complex Formation at Lower Concentration of Amorphous Aluminosilicate

In soil systems, the concentration of solid in the solid–liquid interfacial reactions is assumed to be ranging quite widely. While the solid phase is predominant in upper part of soils, concentration of solid is quite low in aquifer and spring water. Solid–liquid interfacial reactions with low concentration of solid are assumed to contribute significantly to determine the composition of river and ground water. However, there is little information concerning the solid–liquid interfacial reactions with low concentration of solids. Therefore, I studied the reaction between Zn ions and the synthesized amorphous aluminosil–icate maintaining the solid concentration 0.1 g / L, ten times lower than the solid concentration used in the previous section.

Figure 3–7 shows the relationship between the absolute amount of Zn re–tained by amorphous aluminosilicate and the absolute amount of H^+ released from the solid phase. As a whole, the plotted result fits a line with a slope 2. This slope can be explained by the surface complex formation between one Zn^{2+} ion and two –OH groups on the surface of the amorphous aluminosilicate as shown in Eq. [3–2].

$$2\{\text{Al, Si–OH}\} + Zn^{2+} = \{(\text{Al, Si–O})_2\text{Zn}\} + 2H^+. \qquad [3\text{–}2]$$

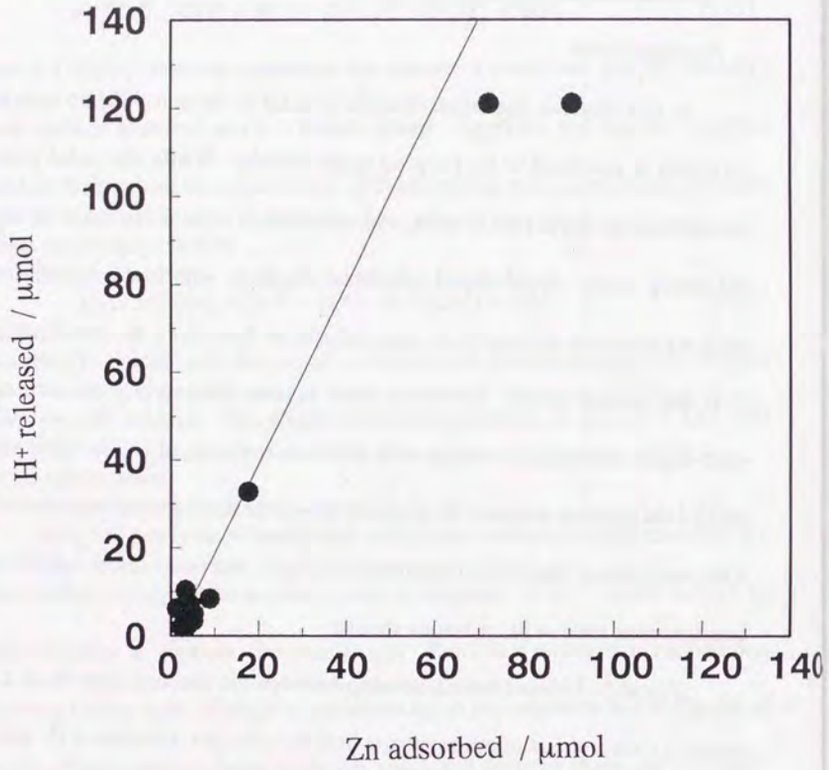

Figure 3–7 Relationship between the amount of Zn adsorbed onto amorphous aluminosilicate and H^+ released from the solid phase. (The range of adsorbed amount of Zn is up to 100 μmol.) The solid line shows a slope of 2.

This result is consistent with the results obtained by experiment using 1 g / L suspensions (Fig. 3–5, 3–6).

In the experiment, the total concentration of Zn in the reacting suspension was increased by an almost constant interval. However, the adsorbed amount of Zn did not increase constantly (Fig. 3–7). In Fig. 3–7, it can be seen that the amount of adsorbed Zn increased suddenly after exceeding 10 μmol. This result clearly points out that the observed solid–liquid interfacial reaction did not involve a single mechanism, because if the reaction occurred by a single mechanism, a sudden increase should not be observed. By the previous experiment using 1 g / L suspension, a linear relationship was confirmed between the total concentration of Zn and the amount of Zn adsorbed by 1 g of solid (Fig. 3–4), when Zn was adsorbed onto the surface by a single mechanism.

An expanded graph of the lower concentration part of Fig. 3–7 is depicted in Fig. 3–8 in order to examine the mechanism of the solid–liquid interfacial reaction. In Fig. 3–8, the resulting points do not remain around the line with a slope of 2 (dotted line), but are spread around a line with a slope of 1 (solid line). This result shows that one Zn adsorption releases one H^+ ion, rather than two H^+ ions. The slope determined from our data given in Fig. 3–8 by the least–squares method was 0.84 ± 0.19. The correlation coefficient was 0.87. These calculations suggest that Zn is adsorbed onto the surface of amorphous aluminosilicate by some other mechanism than that expressed by Eq. [3–2]

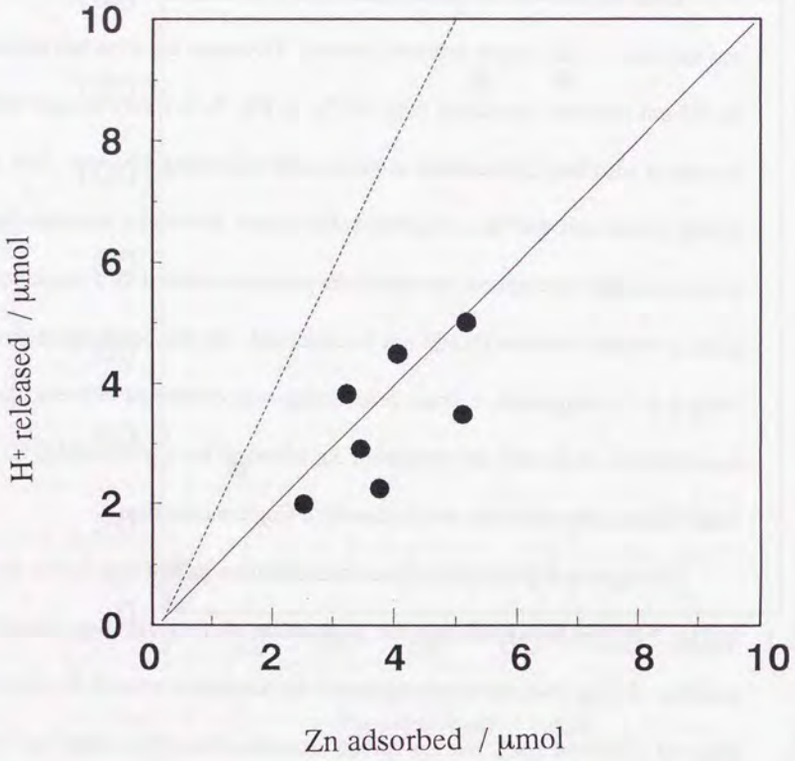

Figure 3–8. Relationship between the amount of Zn adsorbed onto amorphous aluminosilicate and H^+ released from the solid phase for the less adsorption region. (The range of adsorption amount of Zn is up to 10 μmol.) The solid line shows a slope of 1 and the dotted line shows a slope of 2.

when the total concentration of Zn is low.

Figure 3–9 depicts the H^+ released / Zn adsorbed ratio at every total concentration of Zn in the reacting suspension. From Fig. 3–9 it can be seen that there are three regions which depend on the total Zn concentration. The first is region I, where the H^+ released / Zn adsorbed ratio is near 1. This can be seen at a low concentration of the total Zn. The second is region III, where the H^+ released / Zn absorbed ratio is 2. This can be observed at a high concentration of the total Zn. The third is region II, where the ratio is located between the former two. In this region the ratio fluctuates from 1 to 5. The experiment was performed twice, and these three types of regions were observed in both cases.

The Freundlich equation was applied to the result in order to determine what happens on the surface of aluminosilicate (Fig. 3–10). The Freundlich equation is an empirical adsorption isotherm, which is used to describe adsorption phenomena at a solid–liquid interface. The result of the adsorption experiment corresponds to the two lines in Fig. 3–10. In this figure one line corresponds to region I in Fig. 3–9, where the H^+ released / Zn adsorbed ratio is near 1. The other line in Fig. 3–10 corresponds to region III in Fig. 3–9, where the ratio is 2. The crossing region of the two lines in Fig. 3–10 corresponds to region II in Fig. 3–9, where the value of the H^+ released / Zn adsorbed ratio is fluctuating.

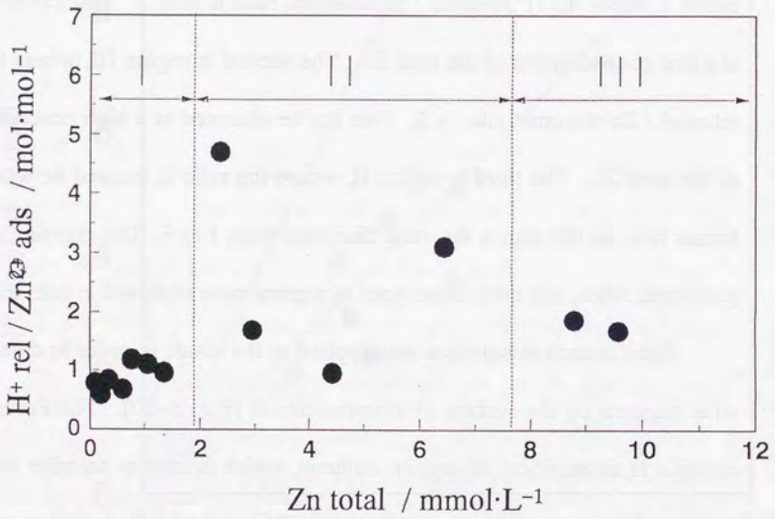

Figure 3–9. Value of the H^+ released ratio to Zn adsorbed at each concentration of total Zn in the reacting system. I, II, and III show different regions depending on the H^+ release / Zn^{2+} adsorption ratio.

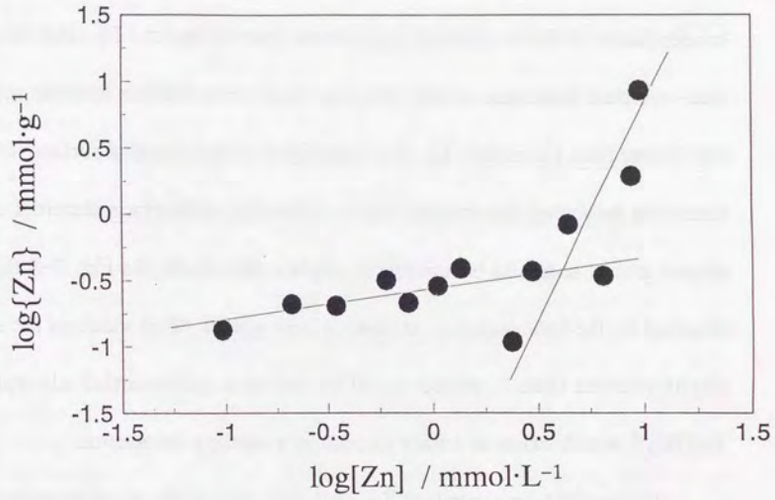

Figure 3–10. Plots according to the Freundlich equation: $\log\{Zn\} = a + b \log[Zn]$. Here, {Zn} means the Zn concentration on the solid (μmol / g), and [Zn] means the Zn concentration in the liquid phase (mmol / L). Both a and b are constants.

From Fig. 3–10, it can be said that there are two kinds of surface–complex formations with different mechanisms between the synthesized amorphous aluminosilicate and Zn ions. These mechanisms change, depending on the total Zn concentration. The surface–complex formation between one Zn^{2+} ion and two surface hydroxide groups, as shown in Eq. [3–2], occurs when the total concentration of Zn is relatively high (more than 1.5 mmol / L). The other surface–complex formation occurs when the total concentration of Zn is relatively low (lower than 1.5 mmol / L). It is reasonable to suppose that surface–complex formation between a monovalent Zn–complex ion and surface aluminol and / or silanol groups seems to be suitable to explain this result. In Fig. 3–8 the slope obtained by the least–squares method is 0.84 ± 0.19. This value of the slope is slightly lower than 1, which could be due to a preferential adsorption of $Zn(OH)_2^0$, which exists as a trace amount in a reacting suspension.

The possible monovalent Zn–complex ions in the reacting solution are $Zn(OH)^+$ and $Zn(NO_3)^+$. The relative possibility for the presence of the Zn ion species in the reacting condition can be calculated as follows using the equilibrium constants listed in Table 3–1:

$$Zn^{2+} : Zn(NO_3)^+ : Zn(OH)^+$$

$$= \quad 1 \quad : \quad 0.25 \quad : \quad 0.03. \qquad [3–3]$$

Although the surface–complex formation of the monovalent Zn ion has not been confirmed experimentally, a few references have mentioned the possi–

Table 3–1. Equilibrium constants used in the calculation (at 25°C) (Kiekens 1990)

Reactions	log K°
$Zn^{2+} + OH^- = Zn(OH)^+$	-7.69
$Zn^{2+} + NO_3^- = Zn(NO_3)^+$	0.40

bility of monovalent Zn ion as being a reacting species. Shindler (1981) has pointed out that monovalent Zn ions (e.g., $Zn(OH)^+$, $Zn(NO_3)^+$) may be sorbed in preference to divalent Zn ions, because the solvation energy resisting sorption is smaller for these monovalent species, and the electrostatic repulsion between them and the solid is smaller, when the solid has a positive surface. The synthesized amorphous aluminosilicate which was used in this study has a positive surface in the reacting suspension, because the pH value of this suspension was lower than pH_{ZPC} (see Table 2-1). The electrostatic repulsion between solid surface and the monovalent Zn ion should be smaller than for the divalent Zn ion in my experimental system, too. Therefore, I consider that the monovalent Zn ions were sorbed on the synthesized amorphous aluminosilicate.

Some discussions in reported papers support the above discussion, which indicate the possibility of surface-complex formation of the monovalent Zn ion. For example, Perona and Leckie (1985) have calculated the proton stoichiometry for Cd, Cu, Pb and Zn on $Fe_2O_3 \cdot nH_20$ by a thermodynamic derivation based upon the Gibbs equation. Although they could obtain linear Freundlich isotherms for Cd, Cu and Pb adsorption, they could not obtain a linear isotherm for Zn adsorption. Their results are consistent with my results. This could be explained in terms of two kinds of adsorption mechanisms: one of them is the adsorption of the monovalent complex ion of Zn.

The surface-complex formation with the H^+ released / Zn adsorbed ratio equal to 1 was not observed when the concentration of the solid was higher, i.e., 1 g / L. It is still unclear why the surface-complex formation with the ratio of H^+ released / Zn adsorbed $\approx$ 1 was observed only when the concentrations of both amorphous aluminosilicate and Zn were low (0.1 g / L, lower than 1.5 mmol / L, respectively). However, the results suggest that for surface-complex formation it is necessary to consider the variety of chemical species of heavy metal ions, especially when the concentrations of both the solid and heavy metal are low. These conditions are very similar to those of natural surface-water systems.

In conclusion, it has been found that one H^+ is released by one Zn ion retained on the surface of amorphous aluminosilicate when the concentration of both the solid and Zn are low. This suggests the possibility of surface complexation of such monovalent Zn ions as $Zn(NO_3)^+$ and $Zn(OH)^+$. From the relative possibility for the presence of the Zn ion species shown in Eq. [3-3], the complex formation of $Zn(NO_3)^+$ seems to be reasonable to explain the surface-complex formation with the ratio of H^+ released / Zn adsorbed $\approx$ 1. The surface complex formation can be described as below;

$$\{Al, Si\text{-}OH\} + Zn(NO_3)^+ = \{(Al, Si\text{-}O)\ Zn(NO_3)\} + H^+. \qquad [3\text{-}4]$$

In natural aquatic systems, the concentrations of both heavy metals and solids are usually very low. It is therefore necessary to consider a variety of

mechanisms for surface-complex formation of heavy metal ions depending on the active metal-ion species.

(3) Solid-liquid Interfacial Reaction at Different Sites

The solid-liquid interfacial reactions between the synthesized amorphous aluminosilicate and Zn ions could be described as shown in Eq. [3-2] and [3-4].

$$2\{Al, Si-OH\} + Zn^{2+} = \{(Al, Si-O)_2Zn\} + 2H^+. \quad [3-2]$$

$$\{Al, Si-OH\} + Zn(NO_3)^+ = \{(Al, Si-O)\ Zn(NO_3)\} + H^+. \quad [3-4]$$

In the equations, {Al, Si-OH} means surface aluminol and / or silanol groups. Since Al and Si have different chemical nature, for example electronegativities, aluminol and silanol groups supposed to have different reactivities to the surface complex formation between Zn ions. Okazaki *et al.*,(1989) have reported that the 6-coordinated aluminum is the active site on amorphous aluminosilicates. However, it is still unclear if there is difference between aluminol and silanol for the surface complex formation between Zn ions, and then which -OH groups on amorphous aluminosilicates is the active site. To clarify the active site on the surface, batch adsorption experiments were performed using aluminosilicates with different Si / Al molar ratios. Al_2O_3 and SiO_2-gel were also used to know if the aluminol and silanol groups on the amorphous aluminosilicate have same properties to those on the simple oxides.

Figure 3-11 shows the relationships between the total concentration of Zn and the amount of Zn adsorbed by 1 g of solids. The different symbols in the figure represent solids with different Si / Al ratios. There is a clear difference between the adsorption features of the solids. In Fig. 3-11, the adsorption tendencies of these solids can be divided into two groups. One is the group shown in closed symbols which adsorbs large amount of Zn ions at low concentration of total Zn (lower than 800 μmol / L). The other is a group shown with open symbols which shows increase of adsorption amount higher concentration of total Zn (higher than 600 μmol / L). The former group is composed of the solids with relatively high contents of Al. On the other hand, the latter group is composed of solids which has relatively low contents of Al but high content of Si. Therefore, it can be said that the difference of adsorption tendencies shown in Fig. 3-11 reflects the composition of solids. It is clear that aluminol and silanol play different roles in adsorption of Zn ions.

To compare the reactivity of aluminol and silanol clearly, batch adsorption experiments were performed using Al_2O_3 and SiO_2-gel respectively. Figure 3-12 and 3-13 shows the relationship between the concentration of total Zn in reacting suspension and adsorbed amount of Zn on 1 g of Al_2O_3 and SiO_2, respectively. The clear difference between these two figures indicates the different chemical properties between aluminol and silanol groups.

Figure 3-12 indicates the existence of at least two kinds of solid-liquid

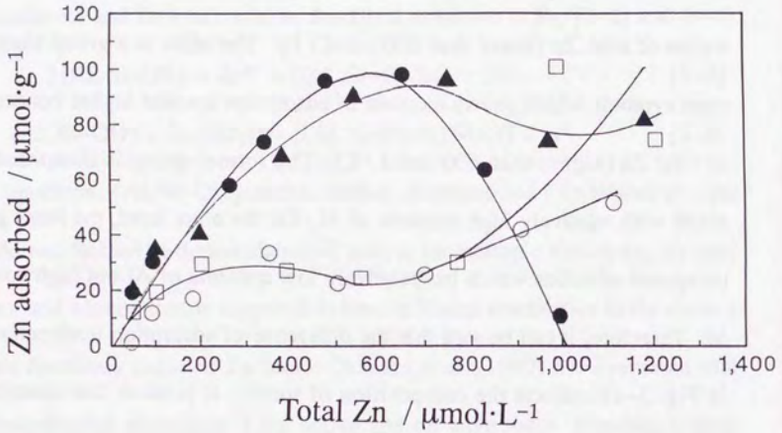

Figure 3–11. Relationship between the total concentration of Zn and the amount of Zn adsorbed by 1 g of solids with different Si / Al ratios. The Si / Al ratios are 0 (●), 0.5 (▲), 1 (□), and 2 (○). The closed symbols represent solids relatively rich in Al and open symbols are used for solids relatively rich in Si.

Si.

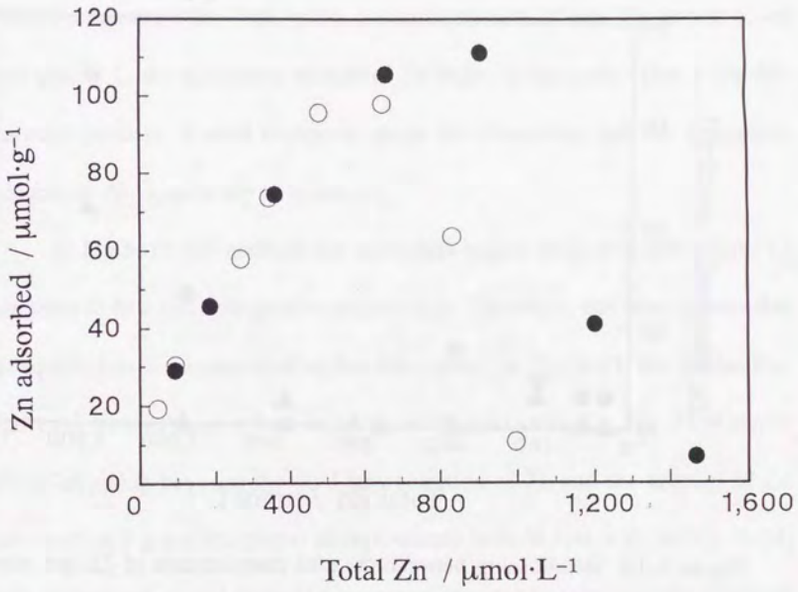

Figure 3–12. Relationship between the total concentration of Zn and adsorbed amount of Zn by 1 g of Al_2O_3. The experiment performed twice and the results of them are severally represented by different symbols.

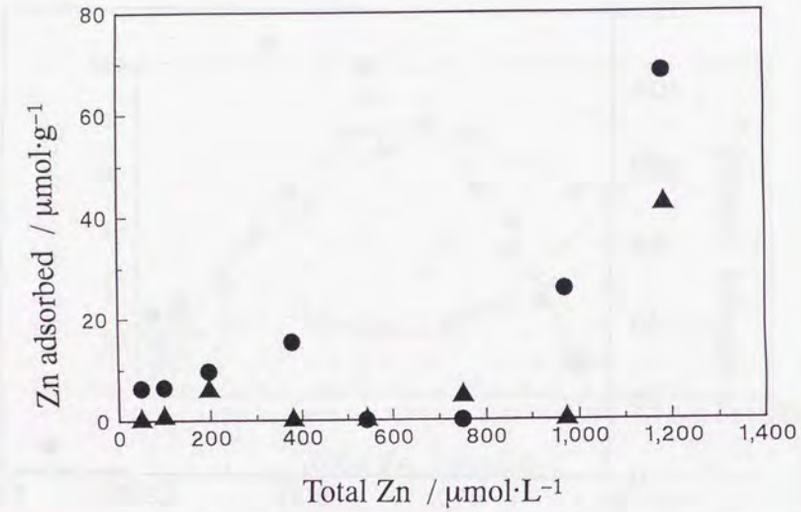

Figure 3–13. Relationship between the total concentration of Zn and adsorbed amount of Zn by 1 g of SiO_2 gel. The experiment performed twice and the results of them are represented severally by different symbols.

interfacial reaction between Zn ions and aluminol groups. One is adsorption and the other is desorption. From Fig. 3–12 it can be seen that Zn ions adsorbed onto Al_2O_3 have linear relationship between concentration of total Zn and adsorbed amount of Zn on 1 g of solid. This reaction has good reproducibility. However, on the other hand, when the concentration of total Zn excess about 600 μmol / L, the adsorption amount of Zn began to decrease. This is the desorption process. I want to discuss about the absorption and the desorption process on Al_2O_3 severally in below.

In Fig.3–12 the results in the adsorption region (from 0 to 600 μmol / L) are seem to fit a line with good reproducibility. Therefore, one may assume that an equilibrium is accomplished within this region. In Fig. 3–11, the similar linearity can be seen more of less for all the solids containing Al. Fig. 3–14 shows the relationship between the total concentration of Zn and the amount of Zn adsorbed on 1 g the amorphous aluminosilicate with Si / Al = 1. In Fig. 3–14, both the adsorption and desorption processes also can be seen, and the results of adsorption region (depicted with closed symbols) fit a line with good reproducibility. Figure 3–15 shows the relationship between absolute amount of adsorbed Zn and released H^+ for the same results shown in Fig. 3–14. In Fig. 3–15, the results depicted with closed symbol, which are the results fitted on a line in Fig. 3–14, gathered on a line with slope 2. This can be explained by a surface

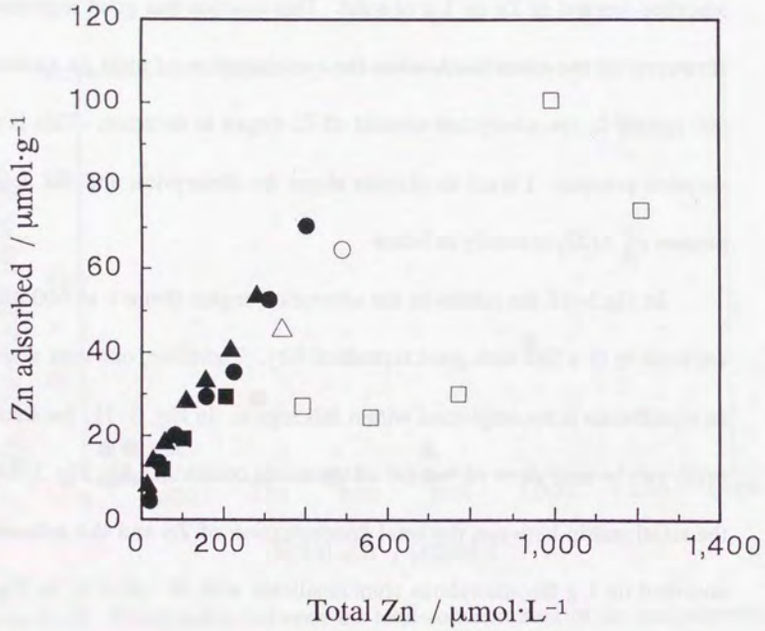

Figure 3–14. Relationship between the total concentration of Zn and adsorbed amount of Zn by 1 g of the synthesized amorphous aluminosilicate with Si / Al molar ratio of 1. The different symbols represent severally the results from experiments using different concentration of Zn stock solutions. The closed symbols are used for the results which seem to fit a line, while open symbols are used for the other.

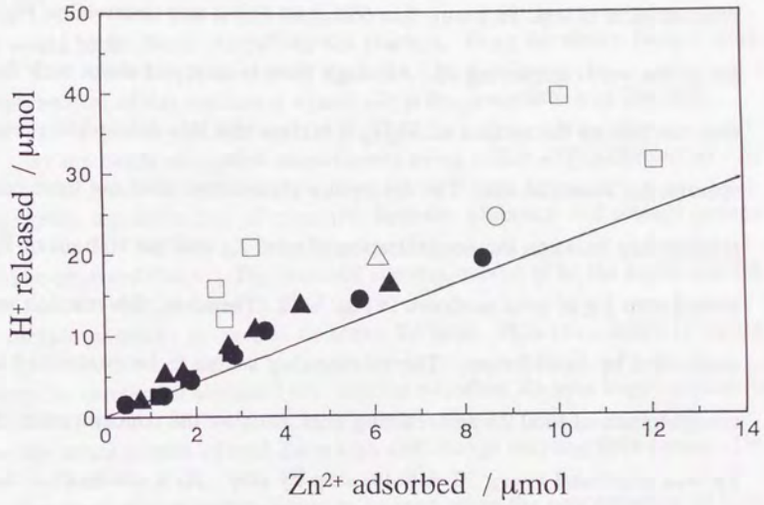

Figure 3–15. Relationship between absolute amount of adsorbed Zn^{2+} and released H^+, which are calculated for the data shown in Fig. 3–14. The type of symbols is followed Fig. 3–14. The line represents a slope of 2.

complex formation between two aluminol groups and one Zn^{2+} ion. Therefore, it seems to be reasonable that aluminol is the active site for the surface complex formation with Zn ion, and the Eq. [3–2] is improved as following;

$$2\{Al\text{–}OH\} + Zn^{2+} = \{(Al\text{–}O)_2Zn\} + 2H^+. \qquad [3\text{–}5]$$

On the other hand, the desorption reaction which can be seen at high concentration of total Zn (more than 600 μmol / L) is also observed in Fig. 3–11 for all the solids containing Al. Although there is no report about such desorption reaction on the surface of Al_2O_3, it is clear that this desorption reaction is specific for aluminol site. The desorption phenomena does not have constant relationship between the concentration of total Zn and the amount of Zn adsorbed onto 1 g of solid as shown in Fig. 3–12. Therefore, this reaction was not controlled by equilibrium. The relationship seems to be controlled by the concentration of total Zn and reacting time, because the concentration of total Zn was increased every 30 minutes step by step. As a mechanism for this desorption reaction, I suppose that Zn, which formed surface complex with aluminol groups, makes soluble complex with Al when the concentration of total Zn is increased, and the rate of this reaction is small, because it doesn't reach equilibrium within 30 minutes.

In Fig, 3–13, we can see solid–liquid interfacial reactions on silanol site. It can be seen that silanol sites do not react with Zn ions until the concentration of Zn excess about 800 μmol / L. In Fig. 3–11, the secondary increase of Zn

adsorption can be seen at higher concentration of total Zn for all the solids which contain Si in their composition. Only Al_2O_3 which has no silanol groups on its surface did not show the secondary increase of adsorption amount. It is clear that this reaction is not controlled by equilibrium. This reaction seems to have a threshold value of the total concentration of Zn, and the reacting time also would be the factor controlling this reaction. From the above facts, I think the mechanism of this reaction at silanol site is the precipitation of $Zn(OH)_2$.

By the batch adsorption experiments using solids with different Si / Al molar ratio, the difference of reactivity between aluminol and silanol groups could be observed clearly. The aluminol site was proved to be the active site for the surface complex formation between Zn ions. However, there is also a desorption reaction at aluminol site, and the adsorbed Zn ions begin to desorb when the concentration of total Zn is high and enough reacting time passes. On the other hand, silanol groups found to be inert when the concentration of total Zn is low and when the concentration of total Zn becomes enough high, $Zn(OH)_2$ precipitation could happen at the silanol site.

The results shown in Fig. 3–11 can be explained by sum of Zn adsorption onto Al_2O_3 (Fig. 3–12) and SiO_2–gel (Fig. 3–13). Therefore, the solid–liquid interfacial reaction between Zn ions and aluminosilicates with different Si / AL ratios can be represented by the sum of the solid–liquid interfacial reaction of

Zn between Al_2O_3 and SiO_2 depending on the surface composition. Fig. 3–11 shows that the solid–liquid interfacial reactions are controlled by the surface composition of solids which reflects the bulk composition.

Usually, the surface of natural soil particles don't have simple composition. For example, natural allophane usually contains iron (Ossaka 1971). It is said that such iron significantly increase adsorption activity of allophane. The result shown in Fig. 3–11 indicated the possibility that we can describe the solid–liquid interfacial reactions of complex oxides by sum of solid–liquid interfacial reactions of simple oxides depending on the surface composition of the complex oxides. Namely, the solid–liquid interfacial reaction between Zn ions and natural allophane could be understand by the sum of reactions between Zn ions and Al_2O_3, SiO_2, and Fe_2O_3 depending on the surface composition. If this possibility is proved, it will be quite helpful for us to understand solid–liquid interfacial reactions in complex soil systems.

3–4 CONCLUSION

A batch adsorption method was newly developed to obtain quantitative information about solid–liquid interfacial reactions between oxides and heavy metal ions. This method enabled to maintain constant values of pH and ionic strength of the reacting suspension, while the concentration of heavy metal ions is varied.

By using the batch adsorption method, the solid–liquid interfacial reaction between Zn ions and the synthesized amorphous aluminosilicate was ascertained to be a surface complex formation between two surface –OH groups and one Zn ion. However, when the concentration of both solid and Zn ions are low in the reacting suspension, a surface complex formation of monovalent Zn–complex ions such as $Zn(OH)^+$ and $Zn(NO_3)^+$ was found.

The different reactivity of aluminol and silanol groups were observed clearly using aluminosilicates with different Si / Al ratios. Aluminol groups were determined to be the active site for surface complex formation of Zn ions. On the other hand, at the silanol sites Zn ions were assumed to precipitate as $Zn(OH)_2$. A possibility was proposed that the solid–liquid interfacial reaction of complex oxide can be described by sum of solid–liquid interfacial reactions of simple oxides depending on the surface composition.

REFERENCES

Anderson, S.J. and Sposite, G. (1991) Cesium-adsorption method for measuring accessible structural surface charge. *Soil Sci. Soc. Am. J.*, **55**, 1569-1576.

Dorfer, K. (1972) *Ion exchange*. Ann Arbert Science, Ann Arbor, MI.

Evans, L.J. (1989) Chemistry of metal retention by soils. *Environ. Sci. Technol.*, **23**, 1046-1056.

Goldberg, S. (1991) Sensitivity of surface complexation modeling to the surface site density parameter. *J. Colloid Interface Sci.*, **145**, 1-9.

Kiekens, L. (1990) Zinc in *Heavy Metal in Soils* (ed.) B.J. Alloway, Blackie, London.

Okazaki, M. and Yamane, I. (1983) 1. Heavy metal absorption to soil components.

Okazaki, M. et al., (1989) Adsorption of ions on synthetic amorphous aluminosilicates with different SiO_2 / Al_2O_3 molar ratios and coordination numbers of aluminum. *Soil Sci, Plant Nutr*. **35**, 109.

Ossaka, J. et al., (1971) Coexistence states of iron in synthesized iron-bearing allophane (Al_2O_3-SiO_2-Fe_2O_3-H_2O system). *Bulletin of the chemical society of Japan*, **44**, 716-718.

Perona, M. J. and Leckie, J. O., (1985) Proton stoichiometry for the adsorption of cations on oxide surfaces. *J. Colloid Interface Sci*. **106**, 64.

Runnels, D.D., Shepherd, T.A., and Angino, E.E. (1992) Metals in water. *Eenviron. Sci. Technol.*, **26**. 2316-2323.

Shindler, P. W., (1981) Surface complexes at oxide-water interfaces in *Adsorption of inorganics at solid-liquid interface*, (eds.) M.A. Anderson and A.J. Rubin, pp.1-49. Ann Arbor Science, Ann Arbor, MI.

Yamamoto, K. (1983) Specific adsorption of zinc and copper by allophane. *Nihon dojyou hiryougaku zassi*, **54**, 519-526.

Ziper, C., Komarneni, S., and Baker, D.E. (1988) Specific cadmium sorption in relation to the crystal chemistry of clay minerals. *Soil Sci. Soc. Am. J.*, **52**, 49-53.

CHAPTER 4: CHEMICAL STATES OF HEAVY METAL IONS AT SOLID–LIQUID INTERFACES

4–1 INTRODUCTION

Knowledge about the chemical states of heavy metal ions on the surface of soil particles is essential to understand the solid–liquid interfacial reactions of heavy metal ions in soil systems. In the previous chapter, I could ascertain the quantitative relationship in solid–liquid interfacial reactions between amorphous aluminosilicate and zinc ions. However, there is no evidence directly proving the formation of chemical bonds between zinc and oxygen atoms in surface hydroxyl groups. In this chapter, spectroscopic methods are applied to analyze the chemical states of ferric and ferrous ions, as well as zinc ions. Iron was selected because it is the most abundant heavy metal in soil (Bowen 1979), one of the main heavy metal in natural water (Runnels et al. 1992), and its movement in soil systems is interesting from a geochemical point of view.

Although spectroscopic analysis of solid–liquid interfaces is quite important, there are few methods to analyze solid–liquid interfaces, because most surface analytical techniques need a high vacuum. In this study, I applied the XAFS (X–ray Absorption Fine Structure) method and Mössbauer spectroscopy to analyze the chemical states of heavy metal ions on the surface of amorphous aluminosilicate. These are rare methods for state analysis of solid–liquid interfaces.

Both the XAFS method and Mössbauer spectroscopy are nondestructive state analytical methods and selective toward a focused element. These methods give us information about the chemical states of atoms of specific elements existing in samples. Therefore, by using these methods, we can distinguish the mechanisms involved in the solid–liquid interfacial reactions of heavy metals: precipitation at the surface, inner–sphere complex formation, and outer–sphere complex formation. If the heavy metal ions form an outer–sphere complex, the chemical state of adsorbed ions will be same as the chemical state of aqua–complex ions. In the case of precipitation at the surface, the chemical state of heavy metal ion will be same to that of hydroxide. When the heavy metal ions are adsorbed on the surface of amorphous aluminosilicate by inner–sphere complex formation, the chemical states of heavy metals can be predicted to be different from both aqua–complex ions and hydroxide. Therefore, in this chapter I used the XAFS method and Mössbauer spectroscopy to compare the chemical states of heavy metal ions adsorbed on the surface of amorphous aluminosilicate with those of aqua–complex ions and hydroxides.

The characteristics of these experimental methods are described below.

(1) XAFS Method

XAFS, a kind of X–ray absorption spectroscopy, is a useful technique to

obtain structural information on materials. The term XAFS includes two different analytical methods (Fig. 4–1): XANES (X–ray Absorption Near Edge Structure) and EXAFS (Extended X–ray Absorption Fine Structure). These two methods have different mechanisms and analytical procedures.

XANES, which refers to the energy region from the pre–edge up to about 50 eV higher than the absorption edge, is related to the excitation of core electrons from an inner shell to empty levels or to the continuum. The analysis of XANES provides information about the oxidation state of the absorber atom, coordination geometry, and the metal–ligand covalence.

On the other hand, EXAFS refers to oscillations of the X–ray absorption on the high–energy side up to about 1 keV above the absorption edge. As a first approximation, EXAFS can be described as an interference effect between the electronic wave emerging from the absorbing atom and the wave being back–scattered by surrounding atoms, once photoelectrons have been ejected by X–ray absorption. Structural information which can be obtained from the analysis of EXAFS spectra includes geometrical parameters such as interatomic distance and coordination numbers around the absorbing atom.

One of the advantages of XAFS over other analytical methods is the fact that XAFS method can apply to samples of any phase. Therefore, it is a quite useful technique in analyzing chemical states at solid–liquid interface. Hayes *et al.* (1987) applied EXAFS to selenium oxyanions and distinguished inner– and

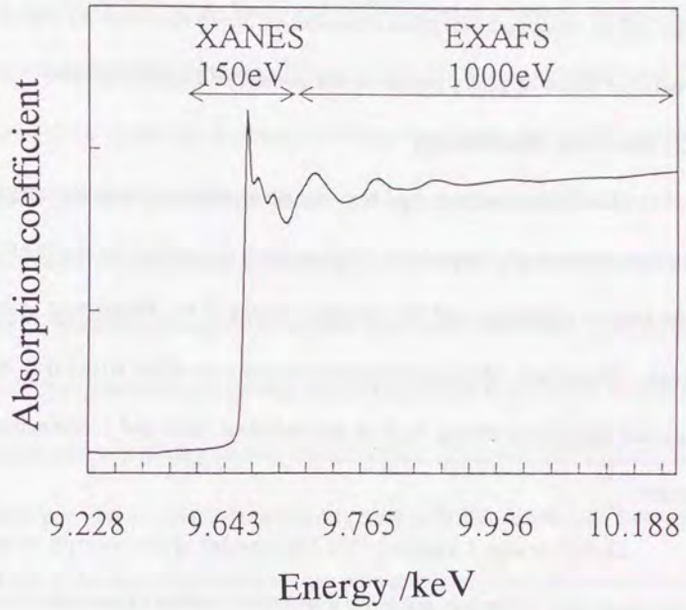

Figure 4–1. Example of XAFS (X–ray Absorption Fine Structure) spectrum. The regions of XANES (X–ray Absorption Near Edge Structure) and EXAFS (Extended X–ray Absorption Fine Structure) are shown.

outer-sphere complexes on an α-FeOOH surface. Recently, Fendorf *et al.* (1994) applied the XAFS method to analyze the chemical state of chromium ions on the surface of silica. Although the XAFS method is being increasingly applied to analyze adsorption phenomena, there has been no report about the chemical states of heavy metals on the surface of aluminosilicate.

(2) Mössbauer Spectroscopy

Mössbauer spectroscopy is γ-ray absorption spectroscopy using recoilless nuclear gamma-ray resonance. This method is sensitive to the configuration of the nearest neighbors and the oxidation states of the Mössbauer atoms in samples. Therefore, Mössbauer spectroscopy can offer structural information around Mössbauer atoms, such as the oxidation state and coordination environment.

In this study, I applied ^{57}Fe Mössbauer spectroscopy to analyze the chemical state of ferrous and ferric ions on the surface of amorphous aluminosilicate. Usually, samples for Mössbauer spectroscopy must be solid, because the Mössbauer atom has to absorb gamma-rays without recoiling. In this study, Mössbauer spectroscopy is applied to frozen samples.

4-2 EXPERIMENTAL

(1) XAFS Method

Samples for XAFS method were prepared by adsorption experiments. Aquatic solutions of $Zn(NO_3)_2$, $FeCl_2$ and $Fe(NO_3)_3$ were prepared in appropriate concentration individually, being adjusted their pH to 6.5, around 6 and 2.5, respectively. The synthesized amorphous aluminosilicate was added to these solutions and obtained suspensions were stirred by a magnetic stirrer for an hour severally. As for the suspension containing Zn^{2+} and Fe^{3+}, the solid phase was separated by filtration using 0.45μm pore size membrane filter (Millipore, HAWPO 4700). The solid phase was washed by water three times to remove heavy metal ions remaining among the particles. The wet solid phase was immediately put into a polyethylene bag together with the membrane filter and sealed. This is the way of preparation for adsorbed samples. However, in the case of Fe^{2+}, special care was necessary to prevent samples from oxidation. Namely, adsorption experiments were performed in N_2 atmosphere and the solid phase was collected by centrifugation. Additionally, the sample was kept in Aneropack (Pouch Kon Bag, Mitusbisi Gas Chemistry), which doesn't let oxygen in, until just before the XAFS measurement in Photon Factory.

In XANES analysis, standard materials are necessary to compare the

figure of spectrum. Therefore, following samples are also prepared for each heavy metal ions: aquatic solutions, hydroxides and samples of adsorbed metal ions on synthesized Al_2O_3 and SiO_2 (Merck, Silica gel 60). The aquatic solutions were severally kept in polyethylene bags with a piece of filter to keep the thickness of samples constant. The hydroxides were obtained by adding NaOH aquatic solution into aquatic solutions containing metal ion, and collected by filtration or centrifugation.

The XAFS measurements were made with synchrotron radiation using a Si(111) channel-cut monochromater at beam line 7C of Photon Factory (PF), Tsukuba. All the samples were analyzed fluorescence detection at room temperature. The incident X-ray intensity was measured with a 17cm-long ionization chamber filled with N_2 gas. For fluorescence detection, a wide angle collector with an ionization chamber, a Lytle detector (EXAFS Co.), was used being filled with Ar gas for both Fe-Kα and Zn-Kα fluorescence detection.

(2) Mössbauer Spectroscopy

To prepare samples for Mössbauer spectroscopy, the same adsorption experiments as the sample preparation for XAFS measurement were performed for both ferric and ferrous ions. The obtained wet solid was put into an acrylic

holder and immediately made frozen by soaking in liquid N_2. For comparison, aquatic solution of $FeCl_2$ and $Fe(NO_3)_3$, and precipitated $Fe(OH)_2$ and $Fe(OH)_3$ were also prepared in the similar way.

The Mössbauer spectra were measured with an Austin Science S-600 Mössbauer spectrometer using a 1.11 GBq ^{57}Co / Rh source. All the spectra were measured at 80K using a cryostat (Torisha Co., Ltd.). The curve fitting of Mössbauer spectra was performed by computer, assuming that all spectra were composed of peaks with Lorentzian line shapes.

4–3 RESULTS AND DISCUSSION

(1) The Chemical State of Zinc Ions

The XANES spectrum of Zn ions adsorbed on amorphous aluminosilicate is shown in Fig. 4–2 (c) together with the spectrum of $Zn(NO_3)_2$ aquatic solution (e) and the precipitation of $Zn(OH)_2$ (a). All the spectra were normalized so as to make maximum absorption 1. When we compare the spectrum of the aquatic solution and the hydroxide precipitation, it is clear that their XANES spectra are completely different, reflecting the difference in the chemical states of Zn in these samples. Therefore, XANES is a useful method in observing chemical states of Zn in wet samples.

In Fig. 4–2, the spectrum of the Zn ions adsorbed on amorphous aluminosilicate is different from those of either the aquatic solution or the hydroxide. This fact means the Zn ions make neither an outer–sphere complex nor a hydroxide precipitation on the surface of the amorphous aluminosilicate. It can be concluded that Zn ions form an inner–sphere complex on the surface of the solid.

In Fig. 4–2, there are also shown spectra of Zn ions adsorbed on Al_2O_3 and SiO_2–gel. When we compare the spectrum of Zn ions adsorbed on amorphous aluminosilicate with these spectra, it can be seen that the spectra of Zn

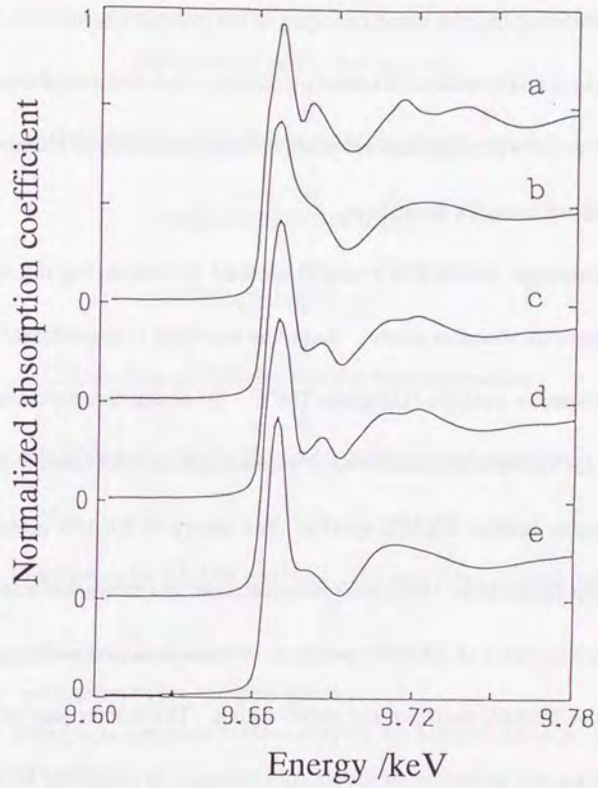

Figure 4–2. XANES spectra of Zn ions (a) in $Zn(OH)_2$ precipitate, (b) adsorbed on SiO_2 gel, (c) adsorbed on the amorphous aluminosilicate, (d) adsorbed on Al_2O_3, and (e) in $Zn(NO_3)_3$ aquatic solution.

ions adsorbed on amorphous aluminosilicate and Al_2O_3 are almost same. This fact shows that the inner–sphere complex of Zn on the surface of the amorphous aluminosilicate has the same structure as the complex formed on Al_2O_3. According to the information obtained by XANES, it is concluded that aluminol is the active site when Zn ions are adsorbed onto amorphous aluminosilicate by inner–sphere complex formation.

Although XANES is a useful method in comparing the coordination atmosphere of absorber atoms, there has not been a standardized method for XANES spectra analysis (Udagawa 1993) . To obtain more quantitative information, for example the coordination number and the inter–atomic distance, it is necessary to analyze EXAFS spectra. The theory of EXAFS already took defined form (Stern et al. 1975) with the systematic use of synchrotron radiation.

The analysis of EXAFS spectra is composed of two main parts: extraction of the EXAFS function and curve–fitting. The former part of the EXAFS analysis, i.e. the extraction of the EXAFS function, is composed of the following steps as shown in Fig. 4–3 (Udagawa 1993, Ozutsumi 1994, Bertagnolli and Ertel 1994). The details of each step are described below following to the process of extracting the EXAFS function of the standard material, $Zn(NO_3)_2$ aquatic solution (Fig. 4–4).

Measurement of spectrum

↓

Extraction of $\mu(E)$: $\mu = \mu_d - \mu_v$

↓

Determination of E_0 and conversion of $\mu(E)$ to $\mu(k)$

↓

Approximation of $\mu_0(k)$

↓

Calculation of $\chi(k)$

↓

Calculation of $\Phi(R)$ by Fourier transformation

↓

Calculation of $\chi_i(k)$ by inverse Fourier transformation

Figure 4–3. Procedures for EXAFS analysis. The meanings of each symbol are listed below.

$\mu_d(E)$: measured spectrum

$\mu_v(E)$: adsorption by co–existing atoms

$\mu(E)$: adsorption spectrum emitted only by the focused atom (a function of energy)

$\mu(k)$: adsorption spectrum emitted only by the focused atom (a function of wave numbers)

$\mu_0(k)$: adsorption spectrum of a focused atom when it exists in isolation

$\chi(k)$: EXAFS function

$\chi_i(k)$: EXAFS function of first coordination shell

$\Phi(R)$: radial structure function

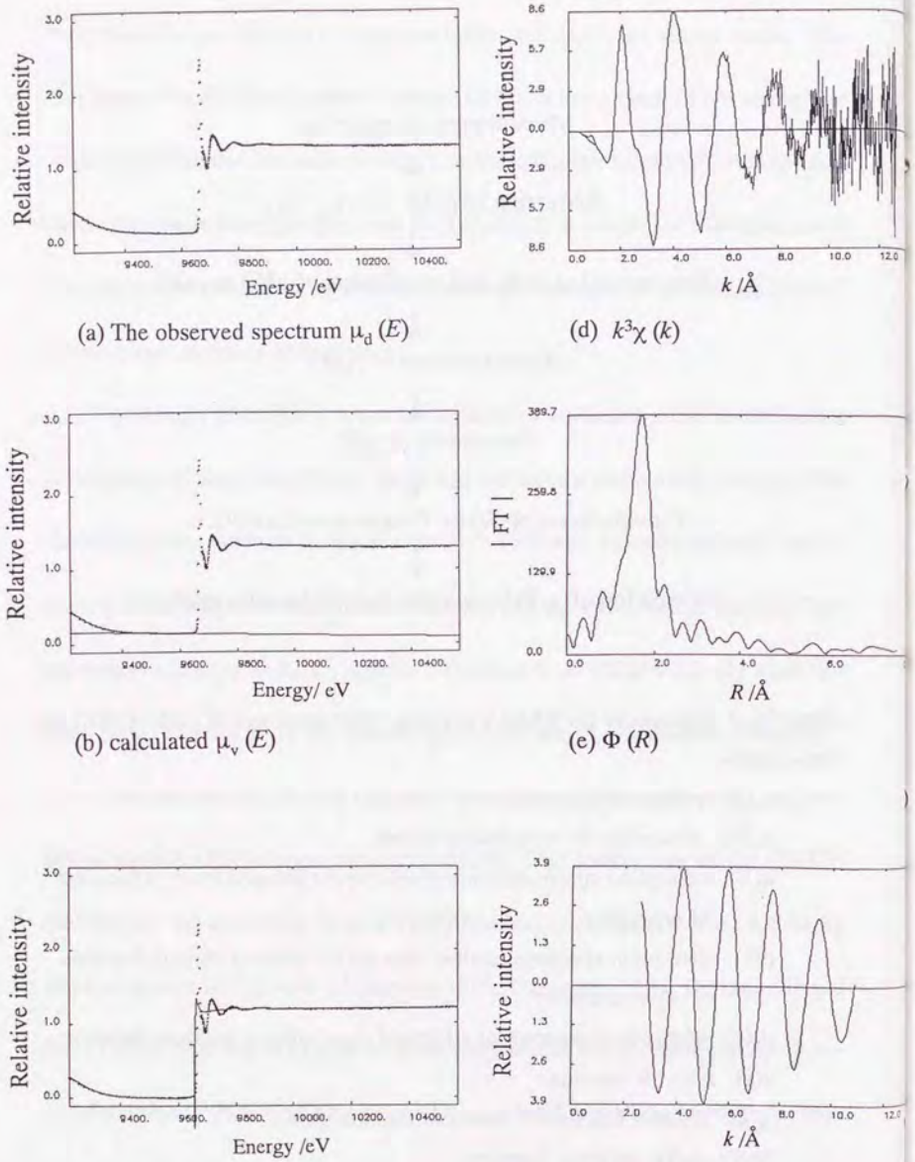

Figure 4–4. Procedure of EXAFS analysis for $Zn(NO_3)_3$ aquatic solution.

(a) *Extraction of* $\mu(E)$. Figure 4–4a is the law spectrum, $\mu_d(E)$, of $Zn(NO_3)_2$ aquatic solution. Since the measured spectrum, $\mu_d(E)$, contains absorption by co–existing atoms, $\mu_v(E)$, it is necessary to extract absorption spectrum emitted only by the focused atom itself, $\mu(E)$. Therefore, $\mu_v(E)$ is calculated from the pre–edge region of $\mu_d(E)$ using Victreen's formula. In Fig. 4–4b, the line drawn under the spectrum is $\mu_v(E)$, which was calculated from the pre–edge region in $\mu_d(E)$ using Victreen's formula with weight k^3. Then $\mu(E)$ is obtained by subtracting $\mu_v(E)$ from $\mu_d(E)$.

(b) *Determination of* E_0. The first energy point of the photon, i.e. the position of the absorption edge, has to be determined in order to calculate the magnitude of the photoelectron wave vector. Using the determined E_0 value, the absorption spectrum can be converted from function of energy, $\mu(E)$, to that of wave numbers, $\mu(k)$.

(c) *Approximation of* $\mu_0(E)$. To obtain the EXAFS oscillation curve $\chi(k)$, it is necessary to obtain $\mu_0(E)$, which is the absorption spectrum of a focused atom when it exists in isolation. $\mu_0(E)$ is approximated by $\mu(E)$ using a polynomial function. $\mu_0(E)$, which is shown by the dotted line in Fig. 4–4c, is approximated using a six–ordered polynomial function for 11.02 ~ 11.85 keV. Then the EXAFS function, $\chi(k)$, is calculated (Fig. 4–4d) using $\mu_0(E)$ and E_0.

(d) *Fourier transformation*. $\chi(k)$ is a function in k space. To obtain the distribution of the backscatterers, $\chi(k)$ is converted into a function in R space, radial structure function $\Phi(R)$, by using a Fourier transformation. In Fig. 4–4d, the region from 2.6 to 10.5 k of the $k^3\chi$ (k) function was extracted and converted into $\Phi(R)$, a radial structure function (Fig. 4–4e).

(e) *Inverse Fourier transformation*. In the obtained $\Phi(R)$, a peak existing over a range of R corresponding to the first coordination shell is extracted. Then the extracted part of $\Phi(R)$ is converted to $\chi_i(k)$ function by a inverse Fourier transformation. $\chi_i(k)$ is the EXAFS function generated by the first coordination shell. In Fig. 4–5e, the peak existing from 1.55 to 2.18Å corresponds to the first neighbored atom, oxygen. Therefore, the peak is extracted and converted into χ_i(k) (Fig. 4–5f) by inverse Fourier transform. This $\chi_i(k)$ is the EXAFS function of O in Zn aqua–complex. The above is the procedure to obtain an EXAFS function from an observed spectrum. These procedures are repeated several times until an adequate $\chi_i(k)$ can be obtained. Then we can obtain structural information from the obtained $\chi_i(k)$ by curve–fitting procedure.

Figure 4–5 shows the steps of the curve–fitting. The structural parameters contained in the least square fitting of $\chi_i(k)$ is following five; N (coordination number), R (interatomic distance), λ (mean free pass of electron), σ

Figure 4–5. Procedure for curve–fitting of EXAFS spectra.

1. Curve–fitting of Standerd Material

Fixed Parameter: N

Free Parameters: R, λ, σ, ΔE

2. Curve–fitting of Samples

Fixed Parameters: σ, ΔE

Free Parameters: N', R', σ'

(Debye–Waller like factor), and ΔE (correction value of absorption edge). Among these factors, λ and ΔE are experimental parameters, which depend on experimental condition when a series of spectra were measured. Therefore, in the curve fitting procedure, a standard substance is analyzed firstly to obtain these experimental parameters. As the standard substance, we have to select materials which has similar structure to samples and its coordination number and inter–

atomic distance have been already reported. In this study, I used $Zn(NO_3)_2$ aquatic solution, in which zinc is existing as aqua–complex, as a standard mate–rial. The curve fitting of the standard material is performed to calculate the values of the two experimental parameters, λ and ΔE. Then, using the obtained values of λ and ΔE as fixed parameters, curve fitting is performed for samples to know the values of *N* and *R*. The fitting is performed several times giving possible initial values of non–fixed factors, till the value of R–factor (like error) becomes less than 10%.

Table 4–1 shows the results from the curve–fitting of the EXAFS func–tion of O in aqua–complex of Zn (Fig. 4–4f). As for the aqua–complex of Zn, the reported value for the coordination number and the interatomic distance are 2.1 Å and 6, respectively (Ohtaki and Radnai 1993). Therefore, the curve fitting

Table 4–1. Structural parameters obtained by curve fitting for standard samples, $Zn(NO_3)_2$. *R* was a fixed parameter.

Sample (Standerd)	$Zn(NO_3)_2$ aq.
N	6 (fixed)
R (Å)	2.13
σ	0.035
λ	2.87
ΔE	23.5
R–factor (%)	9.72

was performed fixing the value of N at 6.

In Fig. 4–6, the result of the fitting is compared with the original $\chi_i(k)$. It can be seen that the curve calculated by using the fitting data shown in Table 4–1 reproduce quite well the original curve within the range of fitting (from 5.00 to 10.00 Å). Moreover, the obtained interatomic distance, 2.13 Å, is consistent with the reported value, 2.1 Å (Ohtaki and Randnai 1993), and the R–factor is below 10%. Therefore, the values of experimental parameters, $\lambda = 2.9$ and $\Delta E = 24$, which were obtained by this fitting, can be applied to samples.

By using the obtained experimental parameters, curve fitting was performed for samples and the results are shown in Table 4–2. For precipitated $Zn(OH)_2$, the obtained N was 2.5 and R was 1.97. $Zn(OH)_2$ is known to have five modifications: α, β, ,γ, δ, and ε. Among them, ε–$Zn(OH)_2$ is the most stable under 39°C. ε–$Zn(OH)_2$ is composed of tetrahedrons sharing OH groups, and the interatomic distance between Zn and O is 1.94 to 1.96Å. In Table 4–2, although the obtained value of N for $Zn(OH)_2$ was much lower than 4, the R value was consistent with the reported values. The value of the R–factor, which is slightly above 10%, seems to be connected with the too small value of N.

Since there is no report about the structure of surface complex of Zn, I performed fitting for the spectrum of Zn ion adsorbed on Al_2O_3 by using struc–

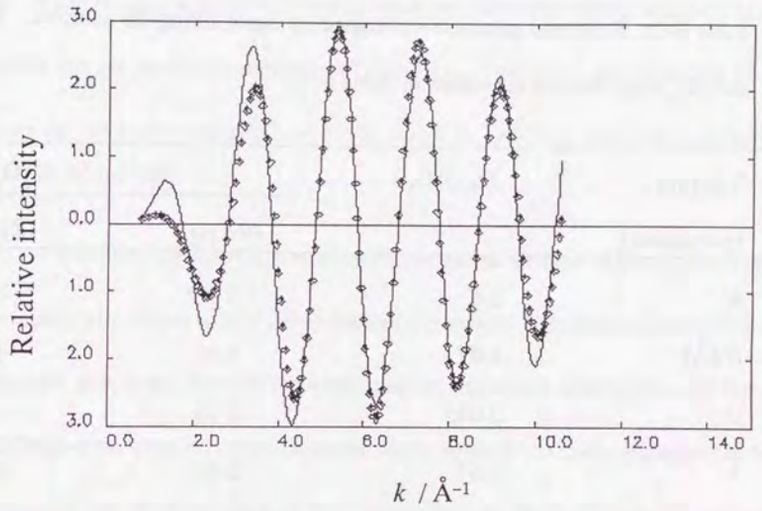

Figure 4–6. Result of curve fitting. The original curve (plotted with ◇) and calculated curve (solid line).

Table 4–2. Structural parameters obtained by curve fitting for samples. The λ and ΔE_0 were fixed at the values in Table 4–1.

Samples	$Zn(OH)_2$	Zn ion on Al_2O_3	
(parameter)		(Zn aq.)	$(Zn(OH)_2)$
N	2.5	5 ± 2	4.96
R (Å)	1.97	1.45	1.97
σ	0.015	0.15	0.044
λ	2.87	2.87	2.87
ΔE	23.5	23.5	23.5
R–factor (%)	13.9	81.5	23.9

(Zn aq) and $(Zn(OH)_2)$ means chemical species, which geometrical parameters were used as initial values in the curve fittings of Zn adsorbed on Al_2O_3.

tural parameters of aqua–complex of Zn and $Zn(OH)_2$ and compared their results. In Table 4–2, the obtained fitting data for Zn ions adsorbed on Al_2O_3 by using the geometrical parameters of the aqua–complex ions of Zn and $Zn(OH)_2$ are shown in the columns titled Zn on Al_2O_3 (Zn aq.) and $(Zn(OH)_2)$, respectively. It can be seen that the R–factor is much smaller when fitting was performed using the geometrical parameters of $Zn(OH)_2$. Therefore, the structure of Zn ions on the surface of Al_2O_3 is much closer to $Zn(OH)_2$ than aqua–complex ions.

It is possible that Zn may polymerize on the surface of amorphous aluminosilicate. Scott *et al.* (1994) studied chromium (III) sorption on silica by EXAFS and found that surface nucleation of chromium hydroxide with the γ–CrOOH–type local structure occurred when surface coverage became greater. However, the Φ (*R*) function of Zn ion adsorbed on Al_2O_3 (Fig. 4–7c) excludes such possibility of polymerization. Since heavier elements contribute to χ (*E*) more significantly, we can see the effect of Zn in Φ (*R*) if the Zn ion is existing as a second neighbor making a Zn – O – Zn bond. In Φ (*R*) of $Zn(OH)_2$ (Fig. 4–7a), the clear peak around 3 Å is caused by a Zn atom existing as a second neighbor beyond the O atom. In Φ (*R*) of Zn ions adsorbed on SiO_2 gel (Fig. 4–7b), there is also a peak around 3 Å. This indicates some extent of polymeriza–

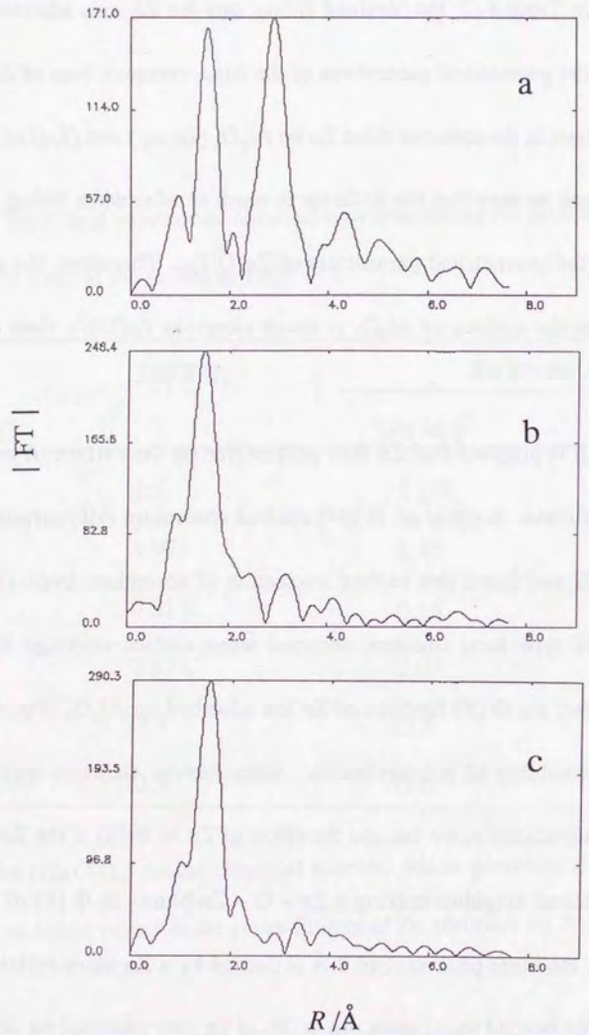

Figure 4–7. Radial distribution functions of Zn ions

(a) in $Zn(OH)_2$ precipitate, (b) adsorbed on SiO_2 gel, and (c) adsorbed on Al_2O_3

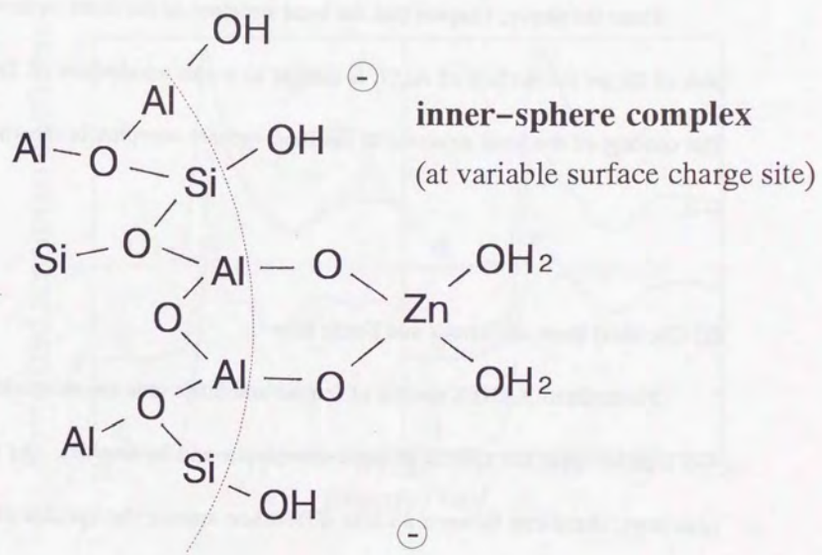

Figure 4–8. Proposed structure of zinc ion adsorbed on the surface of amorphous aluminosilicate.

tion occurred on the surface of the SiO_2–gel. However, there is no peak at 3 Å in the Φ (R) of Zn ions adsorbed on Al_2O_3. Therefore, polymerization of Zn ions did not occur on the surface of Al_2O_3.

From the above, I expect that the local structure of the inner–sphere complex of Zn on the surface of Al_2O_3 is similar to a unit tetrahedron of $Zn(OH)_2$. The concept of the local structure of the inner–sphere complex is shown in Fig. 4–8.

(2) Chemical State of Ferrous and Ferric Ions

Normalized XANES spectra of ferrous and ferric ions are shown in Figure 4–9 together with the spectra of aqua–complexes and hydroxides. As for ferrous ions, there can be seen a clear difference among the spectra of aqua–complex (a), hydroxide (c), and ions adsorbed on amorphous aluminosilicate (b). However, it is not possible to conclude that ferrous ions form an inner–sphere complex on the surface of aluminosilicate, because the XANES spectrum of adsorbed ferrous ion has an absorption edge at a significantly higher energy than does aqua–complex and hydroxide. In XANES spectra the position of the absorption edge gives information about the oxidation state of the absorber atoms. If the absorption edge shifts to a higher energy level, it means the ab–

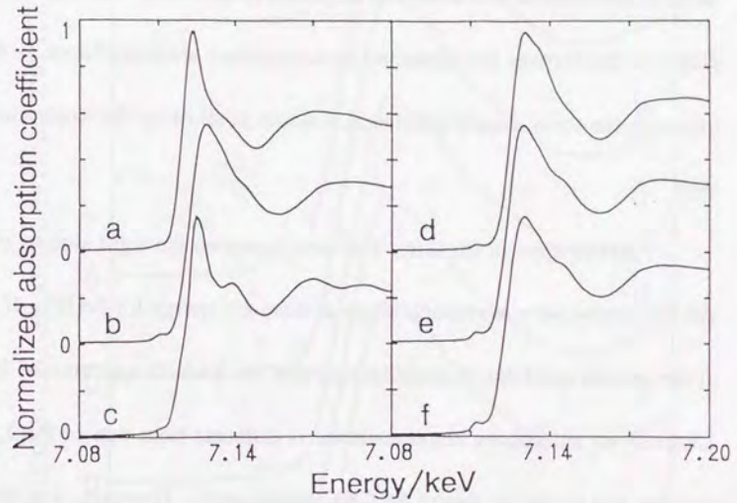

Figure 4–9. XANES spectra of ferrous ions (a) in $FeCl_2$ aquatic solution, (b) adsorbed on the amorphous aluminosilicate, (c) in $Fe(OH)_2$ precipitate, and ferric ions (d) in $FeCl_3$ aquatic solution, (e) adsorbed on amorphous aluminosilicate, (f) in $Fe(OH)_3$ precipitate.

sorber atoms are in a more oxidative condition. The absorption edge in the XANES spectrum of ferrous ion adsorbed on the amorphous aluminosilicate indicates that the ion is oxidized to Fe(III), because the spectrum is almost the same as the spectrum of adsorbed ferric ion (Fig. 4–9e). Therefore, it can be said that the ferrous ion adsorbed on amorphous aluminosilicate is oxidized either by the solid–liquid interfacial reaction itself or by the irradiation of X–rays.

XANES spectra for ferric ions are shown on the right side of Fig. 4–9. All the spectra have absorption edges at adequate energy for Fe(III). If we look at the spectra carefully, it could be said that the XANES spectrum of ferric ion adsorbed on amorphous aluminosilicate is different from that of $FeCl_3$ aquatic solution and similar to that of $Fe(OH)_3$ precipitation. However, it is difficult to see a clear difference among the XANES spectra of samples containing ferric ions.

XANES spectra of ferric ion adsorbed on amorphous aluminosilicate with different loading amounts (Fig. 4–10) also did not show clear differences. Although XANES is useful in comparing the chemical states of zinc, the above results shows that XANES is not so effective for iron. This is due to the nature of the element iron. However, to analyze the chemical states of iron, ^{57}Fe

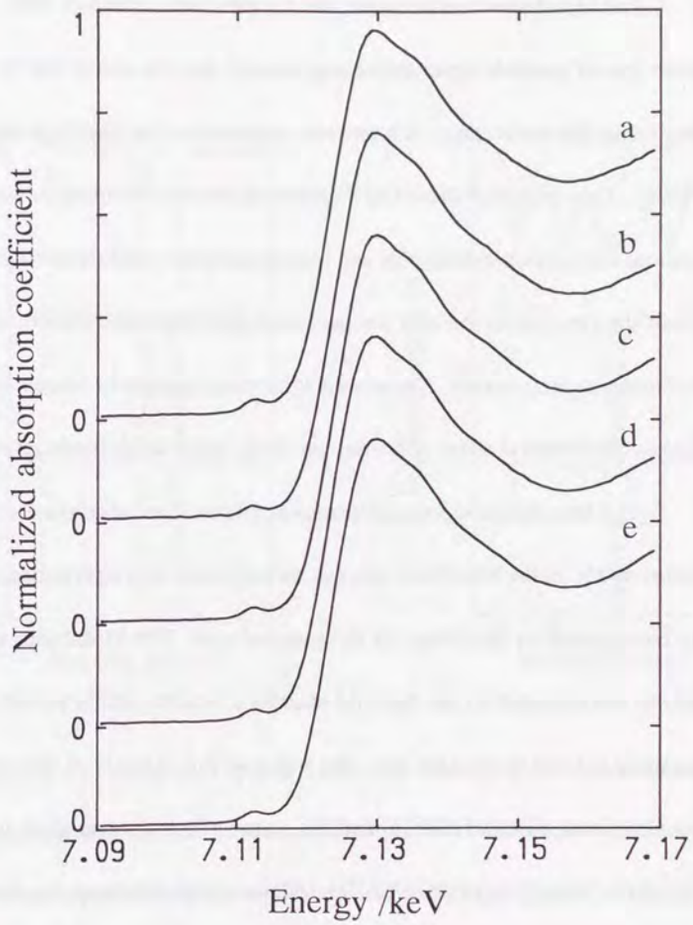

Figure 4–10. XANES spectra of ferric ions on the amorphous aluminosilicate prepared from suspensions with different concentrations of Fe. The samples (a), (b), (c), (d), and (e) were prepared from suspensions with different concentration of Fe: 10, 20, 30, 40 and 50 mmol / L respectively.

Mössbauer spectroscopy can be applied.

For Mössbauer measurement, the samples were frozen at 80K. There is some fear of possible structural change around the iron atoms due to freezing. Regarding this point, there is a previous examination by Manceau and Charlet (1994). They measured the EXAFS spectra of selenate adsorbed on goethite and hydrous ferric oxide at both 80K and room temperature, and reported that analysis of the spectra for the two temperatures gave the same structural results. Referring to their results, I measured Mössbauer spectra of frozen samples to discuss the chemical states of ferrous and ferric ion at solid–liquid interface.

The Mössbauer spectra of ferrous and ferric ions obtained are shown in Figure 4–11. In the Mössbauer spectra, the horizontal axis represented by velocity corresponds to the energy of the gamma–rays. The Mössbauer spectra of ferrous ion adsorbed on the solid (b) showed a doublet similar to that of aqua–complex (a) and hydroxide (c). The value of the velocity at the center of a doublet is called isomer shift (δ) and this value reflects the oxidation state of the Mössbauer atoms. In the case of ^{57}Fe Mössbauer spectroscopy, the larger value of the isomer shift means a more reductive state. In Figure 4–11, all the spectra of ferrous ions have the center of their doublet at the almost same velocity, which corresponds to the value of the isomer shift of high–spin ferrous ions (S =

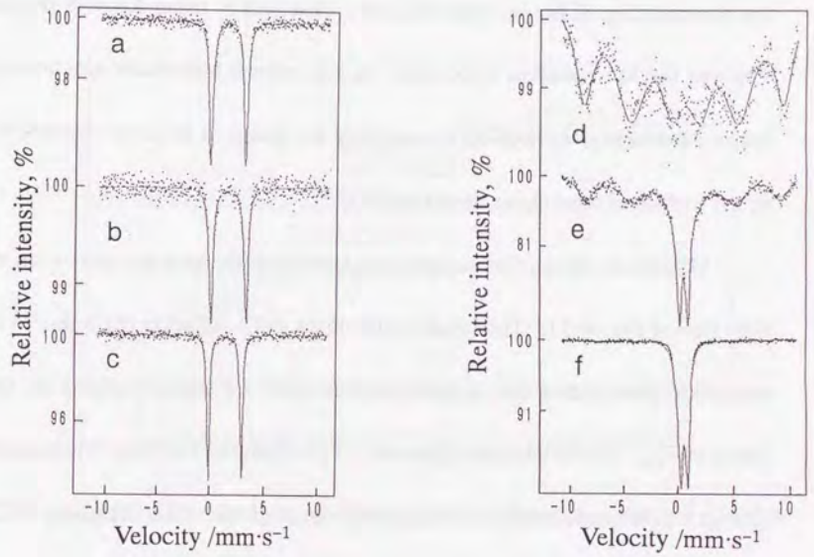

Figure 4–11. Mössbauer spectra for ferrous ions (a) in $FeCl_2$ aquatic solution, (b) adsorbed on amorphous aluminosilicate, (c) in $Fe(OH)_2$ precipitate, and ferric ions (d) in $FeCl_3$ solution, (e) adsorbed on amorphous aluminosilicate, (f) in $Fe(OH)_3$ precipitate.

2) (Fig. 4–12). This means all the iron atoms in the samples are ferrous ions. The ferrous ions on the surface of amorphous aluminosilicate were not oxidized when it was measured by Mössbauer spectroscopy. Therefore, it can be said that the oxidation of ferrous ions which was observed by using XANES (Fig. 4–9 b) was due to irradiation by X–rays. In this respect, Mössbauer spectroscopy has an advantage over XANES in analyzing the chemical states of ferrous ions on the surface of amorphous aluminosilicate.

Mössbauer spectra of samples containing ferric ions are shown on the right side of Fig. 4–11. The broad sextet of the $FeCl_3$ solution (d) is due to the relaxation phenomena that is generally observed for aqua–complex of Fe^{3+} (Sano 1972). The Mössbauer spectrum of precipitated $Fe(OH)_3$ (f) showed a doublet whose isomer shift is in the general range of that of Fe(III) (Sano 1972). The Mössbauer spectrum of ferric ions adsorbed on the amorphous aluminosilicate synthesized (e) has a clear doublet similar to the spectrum of $Fe(OH)_3$ and a trace of a sextet. I think the broad sextet is due to an aqua–complex of ferric ions which remained among the particles after several washings. Since it appears to be impossible to remove the remaining aqua–complex completely, I believe there is an equilibrium between adsorbed ferric ions and aqua–complexes.

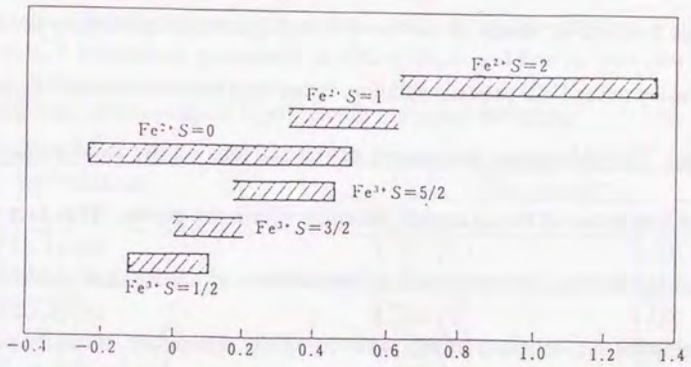

Figure 4–12. Ranges of isomer shifts for chemical states of Fe atom (Sano 1972).

The Mössbauer parameters shown in Table 4–3 are helpful in discussing quantitative factors. In the table, ΔEq means quadruple splitting, which is obtained by the distance of peaks and gives information about coordination symmetry etc. In Table 4–3, ferrous ion adsorbed on the amorphous aluminosilicate has similar values of isomer shift and quadruple splitting to those of ferrous ion in the $FeCl_2$ aquatic solution, rather than those of the $Fe(OH)_2$ precipitation. The Mössbauer parameters of ferrous ions on the solid surface are the same as those of $FeCl_2$ aquatic solution within the errors. This fact indicates that the ferrous ion adsorbed on the surface of amorphous aluminosilicate maintains the structure of the aqua–complex. Therefore, it can be concluded that ferrous ions form an outer–sphere complex on the surface of amorphous aluminosilicate.

On the other hand, ferric ions adsorbed on the amorphous aluminosilicate have similar parameter values to the $Fe(OH)_3$ precipitation. By using Mössbauer analysis, it is possible to deal with all the chemical species of Mössbauer atoms in a sample individually. In Table 4–3, the Mössbauer parameters of the ferric ions adsorbed on the solid are calculated for the doublet in Figure 4–11e. Table 4–3 shows that the ferrous ions adsorbed on amorphous aluminosilicate have larger values for both the isomer shift and the quadruple

Table 4–3. Mössbauer parameters at 80K of ferric and ferrous ions adsorbed on amorphous aluminosilicate together with reference materials.

Substance	Parameter	
	δ(mm/s)	ΔEq(mm/s)
$FeCl_2$ aq	1.37 (1)	3.26 (1)
Fe^{2+} adsorbed	1.39 (1)	3.28 (2)
$Fe(OH)_2$	1.28 (1)	3.08 (1)
$FeCl_3$ aq	0.51 (2)	−0.07 (4)
Fe^{3+} adsorbed	0.46 (1)	0.77 (1)
$Fe(OH)_3$	0.45 (1)	0.65 (1)

The errors in the least significant figure are given in parentheses.

splitting than those of the $Fe(OH)_3$ precipitation.

Takeda *et al.* (1979) studied the chemical states of iron in synthesized allophane by Mössbauer spectroscopy and found that there are two kinds of ferric ions in allophane; ferric ions in a lattice substituting for aluminum, and ferric ions in $Fe(OH)_3$. I can not compare their Mössbauer parameters with those shown in Table 4–3 directly, because their measurements were performed at room temperature. However, according to their report, the ferric ions in the allophane structure have a larger isomer shift than those in $Fe(OH)_3$. Since the amorphous aluminosilicate which is used in this study was characterized as an allophane–like material, the higher value of the isomer shift for the adsorbed ferric ion could indicate that the ion is in a six–coordinate site on the surface of aluminosilicate. The increase in the value of quadruple splitting for the ferric ion adsorbed on aluminosilicate would be explained by a decrease in symmetry.

From the above, it can be said that ferric ion is adsorbed on the surface of amorphous aluminosilicate by inner–sphere complex formation, and the chemical state of the ferric ion in the surface complex is similar to the ferric ion which has replaced aluminum in the six–coordinated allophane structure.

I tried to ascertain the quantitative relationship between the amount of adsorbed Fe^{3+} and released H^+ using the same batch adsorption experimental

method described in Chapter 3. The experiment was performed maintaining the pH value of the suspension constant at 2.5 and varying the concentration of Fe^{3+} from 0 to 0.15 mmol / L. However, I could not ascertain any quantitative relationship (Fig. 4–13). Maybe polymerization of Fe^{3+}, which could happen in the reacting suspension, made it impossible to obtain a constant ration between the H^+ released and the Fe^{3+} adsorbed.

From the above–mentioned results obtained by Mössbauer measurements, I described the chemical states of ferrous and ferric ions on the surface of the synthesized amorphous aluminosilicate in Fig. 4–14. Although the ferric ion is described forming a bidentate complex in Fig. 4–14, the geometry of the inner–sphere complex formed is still unclear. To obtain the geometrical information, it will be necessary to apply EXAFS to this system in the future.

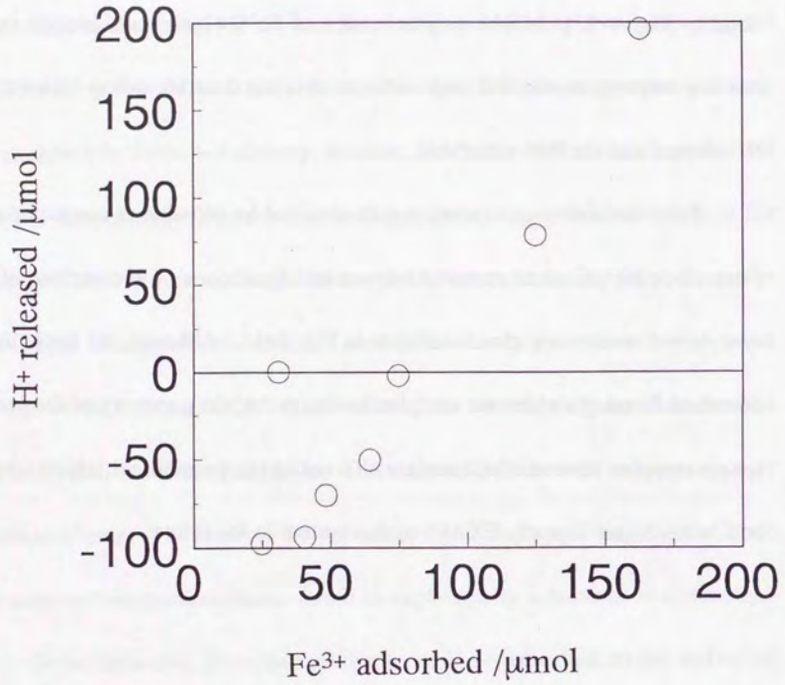

Figure 4–13. Relationship between the absolute amount of adsorbed Fe^{3+} and the absolute amount of H^+. The value of pH was 2.5.

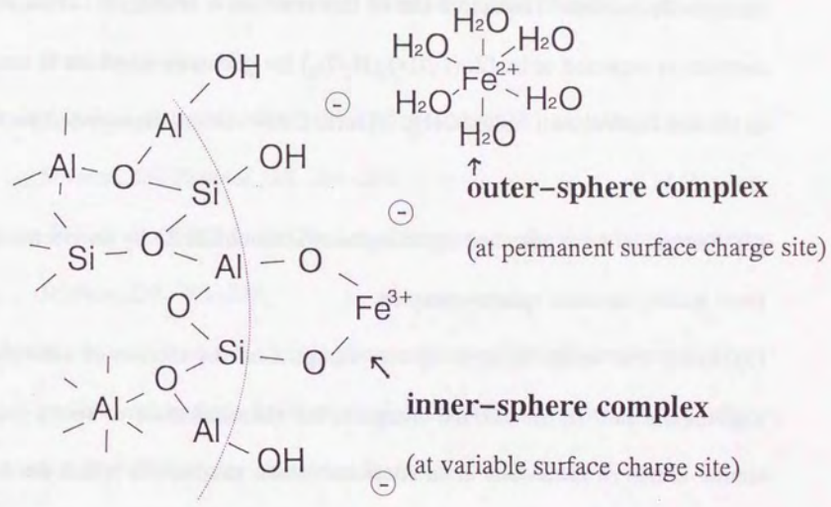

Figure 4–14. Proposed structure of ferric and ferrous ions adsorbed on the amorphous aluminosilicate.

4–4 CONCLUSION

Using the XAFS method and Mössbauer spectroscopy, the chemical state of heavy metal ions at solid–liquid interface were clarified as follows.

(1) Zinc ions are adsorbed on amorphous aluminosilicate by an inner–sphere complex formation. The active site of this reaction is aluminol. The surface complex is expected to be $[Zn(OAl=)_2(H_2O)_2]$ the geometry of which is similar to the tetrahedral unit in $Zn(OH)_2$. (Here, OAl= means dissociated surface aluminol.)

(2) Ferrous ions are adsorbed on amorphous aluminosilicate by an electrostatic force making an outer sphere–complex.

(3) Ferric ions make an inner–sphere complex on the surface of amorphous aluminosilicate. In the surface complex, the chemical state of ferric ions is similar to that of ferric ions in an allophane lattice structure in which the ferric ions substitute for aluminum.

REFERENCES

Bertagnolli, H. and Ertel T.S. (1994) X–ray absorption spectroscopy of amor phous solids, liquids, and catalytic and biochemical systems – capabilities and limitations. *Angew. Chem. Int. Ed. Engl.*, **33**, 45–66.

Bowen, H.J.M. (1979), *Environmental Chemistry of the Elements*, Academic Press, London, p.333.

Fendorf, S.E. et al. (1994) Mechanisms of chromium(III) sorption on Silica. *Environ. Sci. Technol.*, **28**, 284–289.

Hayes, K.F. et al., (1987) In situ X–Ray absorption Study of Surface complexes. *Science*, **238**, 783–238.

Manceau, A. and Charlet, L. (1994) The mechanism of selenate adsorption on goethite and hydrous ferric oxide. *J. Colloid Interface Sci.*, **168**, 87–93.

Ozutsumi, K. (1994) X–ray absorption fine structure. *Bunseki*, **5**, 40–47.

Runnells et al. (1992) Metals in water. *Environ. Sci. Technol.*, **26**, 2316–2323.

Sano, H, (1976) *Mössbauer spectroscopy – The chemical application*, 2nd ed. Kodansha, Tokyo.

Scott, *et al.*, (1994) Mechanisms of chromium (III) sorption on silica. 1.Cr (III) surface structure derived by extended X–ray absorption fine structure spectroscopy. *Environ. Sci. Technol.*, **28**, 284–289.

Stern, E.A. et al., (1975) Extended X–ray absorption fine–structure technique. III–Determination of physical parameters. *Phys. rev. B.*, **11**, 4836–4845.

Takeda, M et al., (1979) Fe-57 Mössbauer study on the structure of an amorphous mineral:synthetic allophane. *Radiochem. Radioanal. Letters*, **41**, 1-10.

Udagawa, Y, (1993) 1. X-ray absorption fine structure in *X-ray absorption fine structure* (ed.) Udagawa, Y., Gakujyutu-syuppan center, Tokyo.

CHAPTER 5: EFFECTS OF CO_2 PARTIAL PRESSURE IN SOIL GAS ON SOLID-LIQUID INTERFACIAL REACTIONS IN SOIL SYSTEMS

5-1 INTRODUCTION

The gas phase of soils is called soil air. Soil air has quite a different composition from the atmosphere (Table 5-1). The difference is due to the structure of soil, which obstructs gas diffusion, and biological activity in the soil systems. A characteristic of the soil air composition is the high concentration of such gases as N_2O, H_2S and CO_2, which are released in the decomposition of organic substances. Recently, the flux of these gases has begun to be a focus of research, because emission of these gases is thought to be a factor increasing the green house effect (Jenkinson *et al.* 1991). Especially the CO_2 and O_2 exchange process between soil air and the atmosphere is called "soil respiration", and there are many articles about it (Anderson 1982, Ouyang and Boersma 1992, Tsuruta 1994).

On the other hand, there are few reports about CO_2 concentration in soil air. Fernandez and Kosian (1987) measured CO_2 concentration in a spruce-fir forest soil from June to November in New England. They reported that CO_2 concentration in O, B, C horizon are 0.10～0.35%, 0.10～1.25%, 0.20～1.20%, respectively, and the maximum concentration was observed in June and October. Castelle and Galloway (1990) monitored the soil air CO_2 concentration in

two acidic soils for two years in Shenandoah National Park, Virginia. They found that the CO_2 concentration in soil air varies in the range of two orders and there was a strong correlation between CO_2 concentration and soil temperature. Fernandez *et al.* (1994) compared the soil air CO_2 concentration in deciduous and coniferous forests with the concentration 4 to 6 years after harvest. The results of one year monitoring indicated that the soil air CO_2 concentrations may be somewhat similar across a diversity of soil types, forest types, and forest condition at any point in time for northern New England. They reported that soil air CO_2 concentration means ranged from 1023 $\mu L\ L^{-1}$ for the O horizon to 3296 $\mu L\ L^{-1}$ for the C horizon. A steady depth profile of soil air CO_2 concentration increasing from the surface (0.03 %) to just below the roots of plants (1～5 %) was proposed by Bolt and Bruggenwert (1980).

Although knowledge about the CO_2 concentration in soil air is limited, it is clear that the CO_2 concentration of soil air is from 10 to 1000 times higher than the atmosphere (Tsuruta 1992), and additionally that the CO_2 concentration is varied by many factors such as temperature, microbiological activity, mineral composition, and depth.

In soil systems, there are equilibria among its three phases: soil particles, soil water and soil air. Since CO_2 dissolves in water, the concentration of CO_2 in soil air must affect solid–liquid interfacial reactions between soil particles and

soil water. However, there are few studies which discuss solid–liquid interfacial reactions in soil including soil air composition.

Reuss and Johnsonn (1985) predicted that the CO_2 concentration in soil air is an important factor in controlling the ANC (Acid–Neutralizing Capacity) of soils. Although they used a simplified equilibria model for this predication, David and Vance (1989) proved the reasonability of the model by an experiment using a Spodosol B horizon at Lead mountain in Maine. On the other hand, it is reported that the soil water collected had higher pH values than the original soil water because of the degassing of CO_2.

The above reports dealt with the relationship between CO_2 in soil air and soil water composition. However, their discussions are still confined to the range of alkalinity. Alkalinity is the value defined by Eq. [5–1].

$$[Alk] = [HCO_3^-] + 2[CO_3^{2-}] + [OH^-] - [H^+] \qquad [5–1]$$

Alkalinity is a convenient measures for estimating the maximum capacity of natural water to neutralize acidic and caustic wastes without extreme disturbance of biological activities in the water (Stumm and Morgan 1981). However, alkalinity is quite a qualitative parameter and its application is limited to the water in such places as limestone area. Therefore, it is not adequate to discuss the effect of dissolved CO_2 on solid–liquid interfacial reactions in soil systems by referring to alkalinity alone.

There is no report about the effect of CO_2 in soil air on solid–liquid inter–

facial reactions between heavy metal ions and the surface of soil particles. However, I think the seasonal variation of CO_2 in soil air which ranges over two orders could affect the heavy metal behavior in soil systems. Therefore, in this chapter I examine the possibility of CO_2 concentration in soil air affecting zinc adsorption onto amorphous aluminosilicate. Here one may predict two possible mechanisms of CO_2 reaction. One is precipitation of a secondary mineral, zinc carbonate, on the surface of aluminosilicate; and the other is a solid–liquid interfacial reaction between the amorphous aluminosilicate and HCO_3^- or CO_3^{2-} ions.

This chapter is an attempt to examine whether the composition of soil gas can influence heavy metal behavior in soil systems. If such influence does take place, seasonal variation of heavy metal concentration in soil water or spring water composition might be explained by the seasonal variation of CO_2 concentrations in soil air.

5–2 EXPERIMENTAL

(1) Laboratory Experiment

Effects of CO_2 partial pressure to solid–liquid interfacial reactions between amorphous aluminosilicate and Zn ions were studied by applying the batch adsorption method developed in Chapter 3. CO_2 in soil gas dissolves in soil water and provides dissolved CO_2 species such as H_2CO_3, HCO_3^- and CO_2^-. The concentrations of the dissolved CO_2 species are regulated by equilibrium constants which are listed in Table 5–1. Therefore, conversely we can calculate the concentrations of dissolved CO_2 species by a partial pressure of CO_2 in gas phase, which are equilibrated with the liquid phase, by using the equilibrium constants. In the experiments in laboratory, the variation of partial pressure of CO_2 in soil air was simulated by the concentration of dissolved CO_2 species, such as HCO_3^- ion, in the reacting suspension.

The batch adsorption experiments were performed by mixing a stock suspension of the amorphous aluminosilicate, a stock solution of $NaHCO_3$, and a stock solution of $Zn(NO_3)_2$. If one wants to maintain the concentration of HCO_3^- in the reacting suspension at x mmol / L, then 4x mmol / L of $NaHCO_3$ stock solution should be prepared. The ionic strength of the stock solution of $NaHCO_3$ is adjusted to 0.1 by using $NaNO_3$ salt and pH value of this solution is adjusted to 6.50 by HNO_3. In the batch adsorption experiments, the concentration of HCO_3^- was increased by adding y ml of 4x mmol / L $NaHCO_3$ solution

Table 5–1 Equilibrium constants concerning dissolved CO_2 species (Stumm and Morgan 1981).

Reactions	log K°
$CO_2(g) + H_2O = H_2CO_3$	-1.46
$H_2CO_3 = HCO_3^- + H^+$	-6.33
$HCO_3^- = CO_3^{2-} + H^+$	-10.32

together with y ml of Zn aquatic solution and 2y ml of mother suspension of the synthesized amorphous aluminosilicate. By this procedure, the ionic strength, pH value and the concentration of HCO_3^- in the reacting suspension can be maintained constant at 0.1, 6.50 and x mmol / L, respectively. For comparison, experiments were performed without HCO_3^- and without solid. These experiments are necessary to clarify the effects of dissolved CO_2 species to solid–liquid interfacial reaction. When the experiment without HCO_3^- was performed, 0.1 *N* $NaNO_3$ aquatic solution was used for $NaHCO_3$ aquatic solution. As for the experiment without solid, 0.1 *N* $NaNO_3$ aquatic solution was used for the mother suspension of amorphous aluminosilicate.

The above is a series of experiments in which the concentration of Zn and solid in the reacting suspension were maintained constant, while the concentration of dissolved CO_2 was increased step by step. As a variation of the above experimental method, I also performed another series of experiments in which the concentration of dissolved CO_2 species and the solid were maintained constant while only the concentration of Zn was increased.

In both series of experiments, the analytical methods and calculation were followed to the way described in Chapter 3–2. Quantitative relationship between the amount of adsorbed Zn and the concentration of dissolved CO_2 species can be obtained by using the batch adsorption method.

Additionally to the batch adsorption experiments, XANES was applied to obtain information concerning the chemical states of Zn ions at solid–liquid interface under the coexistence of dissolved CO_2. XANES spectra were measured for Zn ions adsorbed onto amorphous aluminosilicate under different concentration of coexisting HCO_3^-. The obtained spectra were compared with those of $ZnCO_3$ precipitation, Zn adsorbed on amorphous aluminosilicate with absence of HCO_3^- ions and aqua–complex of Zn. The details of the measurement and analysis of the spectra were followed the way described in Chapter 4–2.

(2) Sampling in Nature

If partial pressure of CO_2 in soil air significantly affects solid–liquid interfacial reactions in soil systems, seasonal variations of soil water composition should be observed related to seasonal variation of partial pressure of CO_2 in soil air. Therefore, to monitor soil water composition together with CO_2 partial pressure in soil air is another approach to clarify the effects of partial pressure of CO_2 in soil air to solid–liquid interfacial reactions. In this section I tried to analyze concentration of heavy metal ions in soil water concerning with partial pressure of CO_2 in soil air. Since there is no commercial apparatus by which

one can monitor seasonal variation of soil air and soil water composition, I constructed a new sampling system and tried to analyze the composition of soil water and soil air at the same time. The detail of the sampling system is described below.

The schematic diagram of the sampling system is shown in Fig. 5–1. This system was constructed referring to the soil–water sampling system used by Ko *et al.* (1995). A set of five holes with diameter 1.8 cm were made in the soil using an earth auger (Daiki Rika Kogyo Co. Ltd.). The depth of the holes are 10, 20, 30, 40, and 50 cm. Then acrylic tubes with the same diameter as the hole (1.4 cm i.d., 1.8 cm o.d.) were inserted into each hole. The lengths of the acrylic tubes were 17, 27, 37, 47, and 57 cm. At the bottom of every acrylic tube, a porous cup (Daiki Rika Kogyo Co. Ltd.), which is a unglazed pottery cup having the same diameter as the hole (1.4 cm i.d., 1.8 cm o.d., 7 cm length), was settled. On the other hand, the top of every tube sticking out from the ground level is connected to a flask by Tygon tube, which is completely inert to soil water. The flask is made of glass and its volume is 500 ml. The whole sampling system is evacuated by a handy aspirator and closed to the atmosphere. Soil water will extracted through the porous cup by the reduced pressure in the collecting system, and moved into the flask through Tygon tube. The first sampling, i.e. the first evacuation, was performed after a month from the settling of the acrylic tubes in soil, because it is necessary to wait until the tubes are fixed

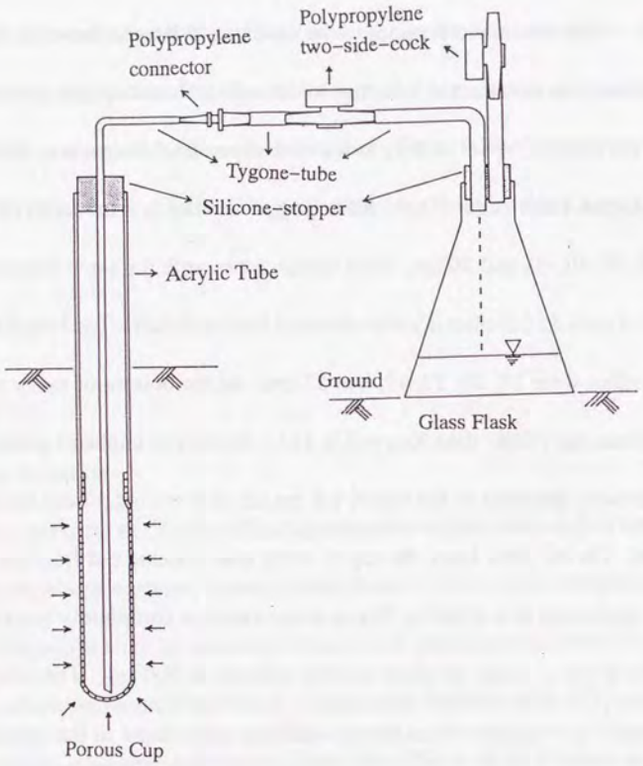

Figure 5-1. Apparatus for soil water and air sampling.

in the soil completely.

The sampling was performed basically every month. After one month the pressure of the gas in the collecting systems increased to almost 1 atom and the gas filling the system can be assumed to have the same composition as the soil gas of the soil around the porous cup. Therefore, the CO_2 concentration of soil air can be obtained by measuring CO_2 concentration of the air in the flask using test tubes. In monthly sampling procedure, CO_2 concentration is measured for the first, and then the system is opened to the atmosphere. The collected soil water in the flasks is moved to polyethylene container and brought to the laboratory. The composition of collected soil water was analyzed by ICP-AES (Inductively Coupled Plasma - Atomic Emission Spectroscopy). By the above method, it is possible to monitor the soil water composition together with the CO_2 partial pressure of the soil air.

The constructed sampling system was tested at Miho forest in Yokohama (Fig. 5-2). A forest was selected to observe clearly the seasonal variation which is mainly due to microbiological activity. Moreover, Miho forest is located near to National Highway 246 and Tomei Expressway, which have heavy traffic as well as two rail ways. Therefore, the forest would be polluted by heavy metals through atmospheric transportation from the traffics. Since the movements of heavy metals in the forest is important for management of water resources,

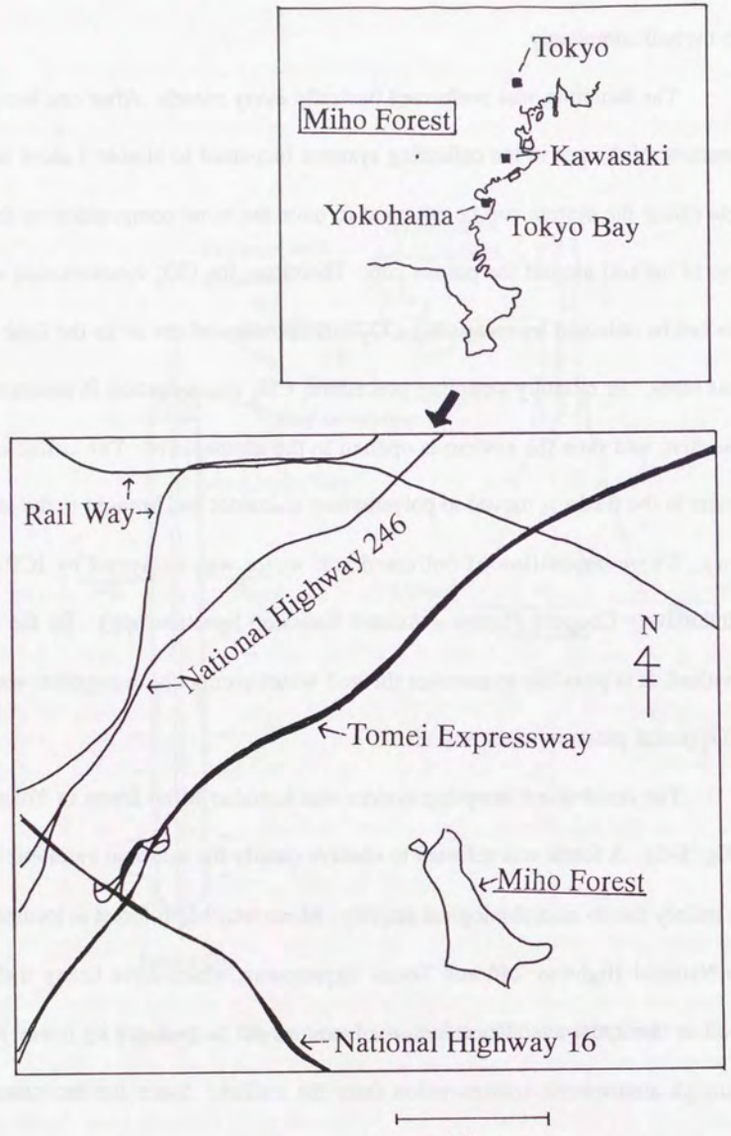

Figure 5–2 Location of the sampling point.

sampling in forest is interesting also from environmental chemistry's point of view.

5–3 RESULTS AND DISCUSSION

(1) Model Experiment

The concentration of dissolved CO_2 species which is equilibrated with CO_2 in soil air can be calculated by the equilibrium constants shown in Table 5–1. The relative abundance of dissolved CO_2 species at pH 6.50 is calculated as follows,

$$H_2CO_3 \quad : \quad HCO_3^- \quad : \quad CO_2^-$$
$$= \quad 40 \quad : \quad 60 \quad : \quad 0.009. \qquad [5\text{–}1]$$

As we can see in Eq. [5–1], the most abundant species is the HCO_3^- ion. Therefore, the dissolved CO_2 concentration, which is the sum of the concentration of H_2CO_3, HCO_3^- and CO_3^{2-}, was determined by the $NaHCO_3$ aquatic solution in the experimental procedure. In the reacting suspension, a part of HCO_3^- added as $NaHCO_3$ aquatic solution will disproponate into H_2CO_3 and CO_3^{2-} according to Eq. [5–1]. However, the total concentration of dissolved CO_2 is the same as the amount of added HCO_3^-, because the experimental system is closed to the atmosphere. As is described in Chapter 3–2, the surface of the reacting suspension is covered with liquid paraffin, and the effect of covering by paraffin can be seen in Fig. 3–2. In the following discussion, I use the amount of added HCO_3^- to the reacting suspension to represent the total amount of dissolved CO_2 species.

The HCO_3^- concentration which is equilibrated with CO_2 partial pressure

in the atmosphere, 340ppm, is calculated to be 0.03 mmol / L at 25 °C and pH = 6.50, using the equilibrium constants shown in Table 5–1. When the partial pressure of CO_2 in soil air is 100 times higher than the atmosphere, the concentration of equilibrated HCO_3^- is 3mmol / L. Since the partial pressure of CO_2 in soil gas is reported to vary seasonally up to more than 100 times that of the atmosphere, the batch adsorption experiments had HCO_3^- concentrations in the reacting suspension ranging up to 5 mmol / L.

Figure 5–3 and 5–4 show the relationships between the absolute amount of adsorbed Zn and released H^+ when the concentration of HCO_3^- was varied 0 0.08 mmol / L and 0 5 mmol / L respectively. In the figures the open circles represent the results with the absence of HCO_3^- for comparison. In both of these experiments, the concentration of Zn was maintained at 0.5 mmol / L. In Fig. 5–3 the results show no clear difference between the experiments with the presence of HCO_3^- and those without it. In both cases the results fit a line with a slope of 2. The region of the HCO_3^- concentration in this experiment corresponds to the partial pressure of CO_2 in the atmosphere. Therefore, it can be said that the surface complex formation between Zn ions and –OH groups on the surface of amorphous aluminosilicate is not affected by CO_2 in soil air when its concentration is as low as in the atmosphere.

On the other hand, in Fig. 5–4 we can see a clear difference between the

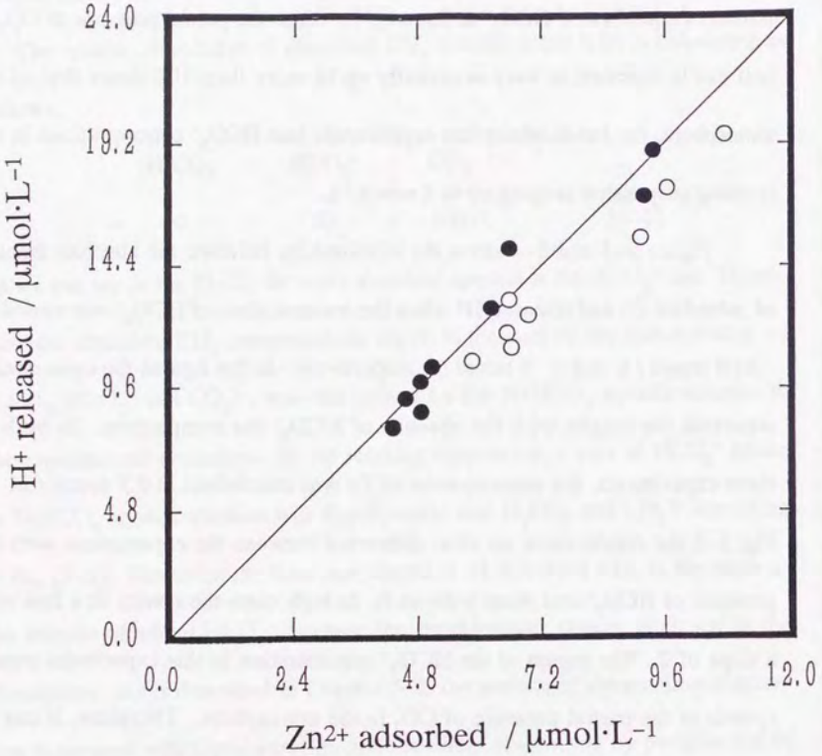

Figure 5–3. Relationship between absolute amount of adsorbed Zn and released H^+ with presence of HCO_3^- (●) and absence of it (○). The concentration of total Zn was maintained at 0.5 mmol / L and HCO_3^- concentration was varied up to 80 μmol / L. The line shows a slope of 2.

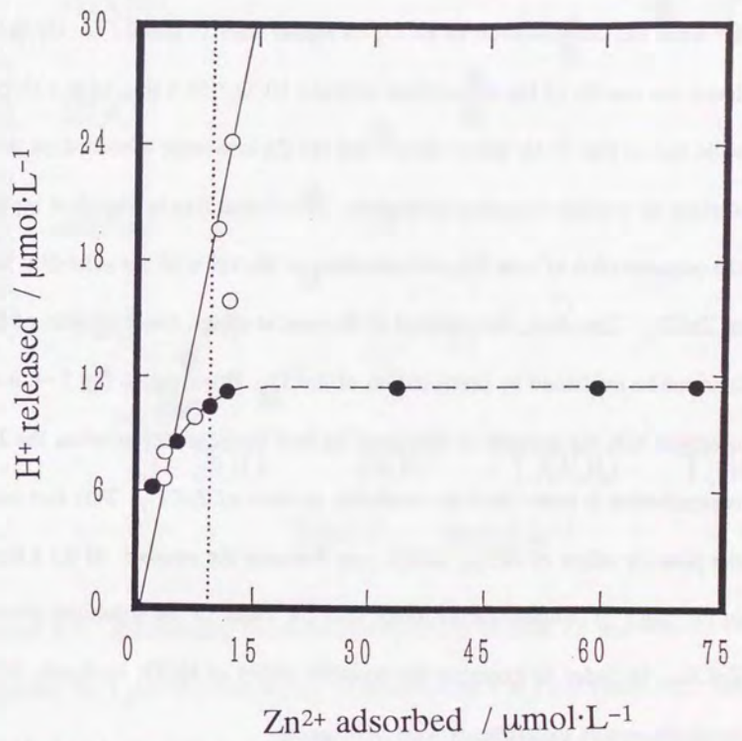

Figure 5–4. Relationship between absolute amount of adsorbed Zn and released H^+ with presence of HCO_3^- (●) and absence of it (○). The concentration of total Zn was maintained at 0.5 mmol / L and HCO_3^- concentration was varied up to 3 mmol / L. The solid line shows slope of 2. The finely dotted line shows a solubility product of $ZnCO_3$.

results with the presence of HCO_3^- and those without it. In this experiment, the highest concentration of HCO_3^- corresponds to the partial pressure of CO_2 about 170 times higher than the CO_2 partial pressure in the atmosphere. In Fig. 5–4, we can see that Zn ions were removed from the liquid phase without releasing H^+ when the concentration of HCO_3^- is higher than 15 μmol / L. On the other hand, the results of the experiment without HCO_3^- fit a line with a slope 2 (a solid line in Fig. 5–4), which shows that the Zn ions were adsorbed on the solid surface by surface complex formation. The dotted line in Fig. 5–4 represents the concentration of total Zn corresponding to the value of the solubility product of $ZnCO_3$. Therefore, the removal of Zn ions at a high concentration of HCO_3^- ions can be explained by precipitation of $ZnCO_3$. However, in Fig 5–4, it can be observed that the amount of adsorbed Zn was increased even when the HCO_3^- concentration is lower than the solubility product of $ZnCO_3$. This fact suggests the possible effect of HCO_3^- which may increase the amount of Zn adsorption in the range of concentrations lower than the value of the solubility product of $ZnCO_3$. In order to examine the possible effect of HCO_3 in detail, different batch adsorption experiments were performed.

In another series of experiments, the concentration of HCO_3^- in the reacting suspension was maintained constant at 2 mmol / L, while the concentration of Zn was increased step by step. Fig 5–5 shows the relationship between concentration of total Zn and amount of Zn adsorbed onto 1 g of the amorphous

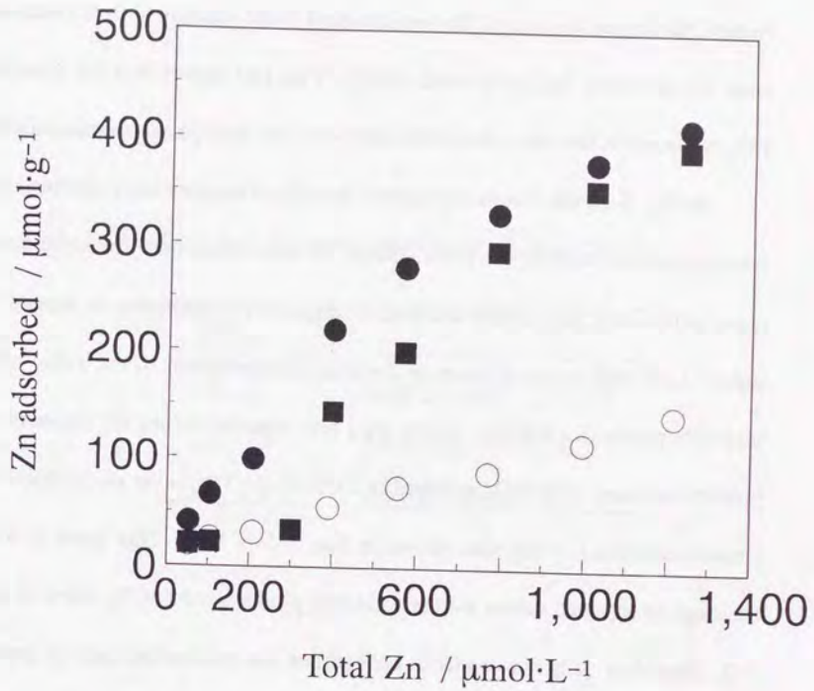

Figure 5–5. Relationship between concentration of total Zn and amount of Zn adsorbed by 1 g of the amorphous aluminosilicate (●) compared with without HCO_3^- (○), and without solid (■). The concentration of HCO_3^- was maintained at 2 mmol / L. The concentration of total Zn was varied up to 1400 μmol / L.

aluminosilicate. It can be seen that in the whole range of total Zn concentration studied, the largest amount of Zn was adsorbed in the reacting system containing both the solid and HCO_3^- (closed circle). This fact shows that the dissolved CO_2 can enhance the adsorption of Zn ions onto the amorphous aluminosilicate.

In Fig. 5–5, the results represented by closed squares were obtained by a reacting system without the solid. Since Zn adsorption onto the solid cannot occur in this case, the sudden increase of apparent Zn adsorption at around 300 μmol / L of total concentration of Zn should correspond to the value of the solubility product of $ZnCO_3$. There are a few reported values for the solubility product constant of $ZnCO_3$ as listed in Table 5–2. The value of the solubility product calculated by the data shown in Fig. 5–5 is 10.4. This value is within the range of reported values for the solubility products of $ZnCO_3$ listed in Table 5–2. Therefore it is reasonable to believe that the sudden increase of apparent adsorption in the system without the solid indicates the value of solubility products of $ZnCO_3$ in the experimental condition.

In Fig. 5–5 the greater amount of adsorbed Zn in the system with the presence of HCO_3^- can be explained by the precipitation of $ZnCO_3$ in the region of total Zn concentration over the value of solubility products obtained above. However, it can be seen that even though the concentration of total Zn is lower than the obtained value of the $ZnCO_3$ solubility product, the amount of Zn

Table 5–2. Reported solubility products of $ZnCO_3$.

pK_{sp}	
10.2	Nagayama (1978)
10.78	Sekine (1980)
10.84	Lange (1973)

adsorption onto the solid is greater with the presence of HCO_3^- than in its absence. This fact suggests that coexisting HCO_3^- can enhance the adsorption of Zn onto the amorphous aluminosilicate. The possible effect of HCO_3^- which was observed in Fig. 5–4 was reconfirmed.

The same experiment was performed at lower concentrations of total Zn and its results are shown in Fig. 5–6. The results shown in this figure agree with those of Fig. 5–5. When the concentration of total Zn is slightly lower than the solubility constant, it can be seen again that the amount of adsorbed Zn is increased specifically in the system containing both the solid and HCO_3^-. Therefore, I could confirm the specific effect of HCO_3^- which enhances Zn adsorption onto amorphous aluminosilicate in the range of Zn concentration slightly lower than the value of the solubility product of $ZnCO_3$. This is the first evidence suggesting that the CO_2 partial pressure in soil air can affect the solid–liquid interfacial reaction of heavy metal ions.

There are two possible mechanisms concerning the effect of HCO_3^- which enhance Zn adsorption onto the solid although the bulk concentration of Zn is lower than the value of the solubility product of $ZnCO_3$. The two different mechanisms are reflecting two different solid–liquid interfacial reactions between HCO_3^- and the surface of aluminosilicate: outer–sphere complex formation and inner–sphere complex formation. If HCO_3^- forms outer–sphere complexes on the surface of aluminosilicate, the increase of Zn adsorption can be

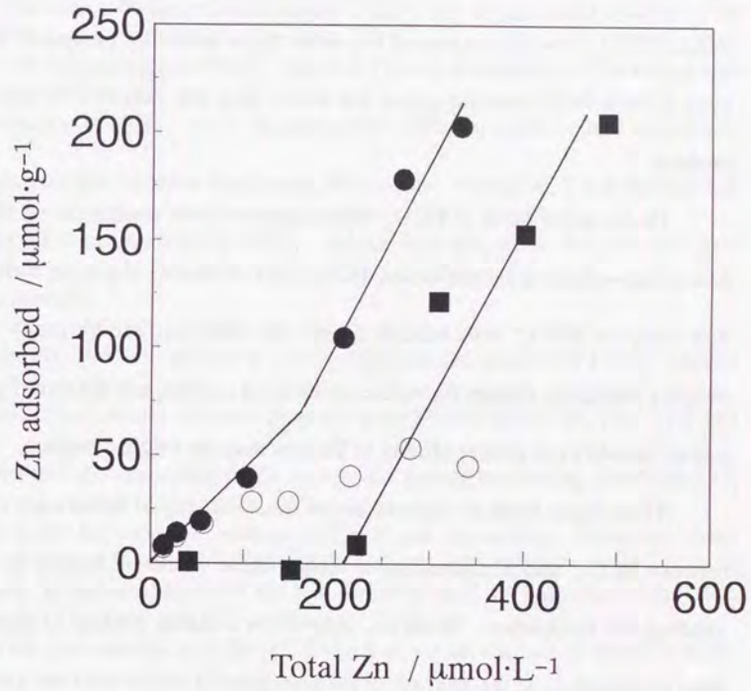

Figure 5–6. Relationship between concentration of total Zn and amount of Zn adsorbed by 1 g of the amorphous aluminosilicate (●) compared with without HCO_3^- (○), and without solid (■). The concentration of HCO_3^- was maintained at 2 mmol / L. The concentration of total Zn was varied up to 600 μmol /L.

explained as precipitation of $ZnCO_3$ on the surface of aluminosilicate. In this case, the concentration of HCO_3^- ions on the surface of the solid is higher than the bulk, because of the outer-sphere complex formation. The local concentrations of HCO_3^- and Zn ion exceed the value of the solubility product of $ZnCO_3$, even if their bulk concentrations are lower than the value of the solubility product.

On the other hand, if HCO_3^- forms inner-sphere complexes on the surface of amorphous aluminosilicate, HCO_3^- acts to modify the solid surface. In this case, the HCO_3^- ions adsorbed onto the solid surface by inner-sphere complex formation change the nature of the solid surface, and the modified solid surface should have greater affinity to Zn ions than the original surface.

There have been no reports about the solid-liquid interfacial reaction between HCO_3^- and aluminosilicate, though these would be helpful in understanding the mechanism. However, XANES is a useful method to distinguish these possibilities. If the increase of Zn adsorption is due to the local precipitation of $ZnCO_3$ on the surface of solid, the XANES spectrum of Zn ions on the surface of amorphous aluminosilicate should be the same as the spectrum of $ZnCO_3$. On the other hand, if Zn ions react with the surface of amorphous aluminosilicate which is modified by HCO_3^-, the XANES spectrum of Zn will be different from the spectrum of $ZnCO_3$.

The obtained XANES spectra are shown in Fig. 5-7. The XANES spectra of Zn adsorbed on amorphous aluminosilicate co-existing with HCO_3^- was measured for samples prepared under different conditions: in systems containing a high concentration of both Zn and HCO_3^- (c); a high concentration of Zn but a low concentration of HCO_3^- (d); and a low concentration of Zn with a high concentration of HCO_3^- (e). In spite of the different experimental conditions, these spectra did not show significant differences. Therefore, it can be said that varying the concentrations of HCO_3^- and Zn does not affect the chemical state of adsorbed Zn.

In Fig. 5-7, the spectra of Zn adsorbed on the solid with HCO_3^- present (c, d, and e) are clearly different from the precipitation of $ZnCO_3$ (b). This fact indicates that the adsorption of Zn ions in the system containing dissolved CO_2 species is not the local precipitation of $ZnCO_3$ on the surface. Moreover, these spectra (c, d, and e in Fig. 5-7) are also different from the spectrum of $Zn(OH)_2$ (f) and the aqua-complex of Zn (g). Therefore, on the surface of the amorphous aluminosilicate, Zn ions are assumed to form inner-sphere complexes. However, this inner-sphere complex is not same as the inner-sphere complex between aluminol groups and Zn ions, because we can see a clear difference between the spectra of Zn adsorbed on the solid in the absence of dissolved CO_2 species (Fig. 4-2 c) and in their presence (Fig. 5-7 c, d, and e).

From the above facts, it can be concluded that dissolved CO_2 species such

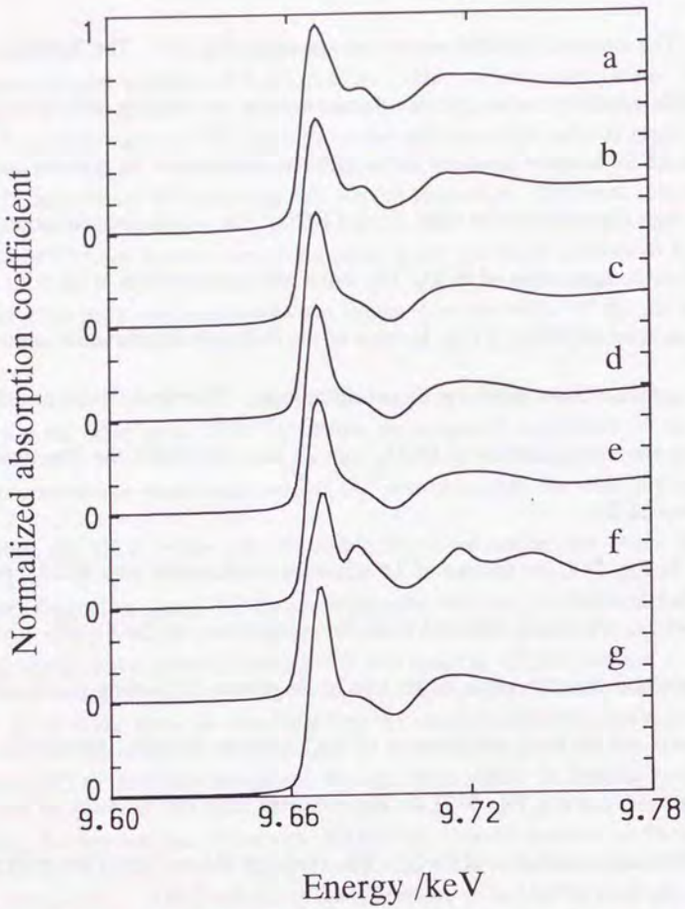

Figure 5–7. XANES spectra of Zn in following samples: (a) $ZnCO_3$ (solid), (b) precipitated $ZnCO_3$ (gel), (f) precipitated $Zn(OH)_2$, (g) aquatic solution of $Zn(NO_3)_2$, and Zn ions adsorbed on amorphous aluminosilicate prepared by suspensions containing (c) high (10 mmol / L) concentration of Zn and high (0.1 mmol / L) concentration of HCO_3^-, (d) high concentration of Zn and low (0.01 mmol / L) concentration of HCO_3^-, and (e) low concentration (1 mmol / L) of Zn and high concentration of HCO_3^-, respectively.

as HCO_3^- ions form inner–sphere complexes on the surface of amorphous aluminosilicate and modify the surface of the amorphous aluminosilicate. Since the modified surface has greater affinity to Zn ions than the original surface, the adsorption of Zn ions onto the amorphous aluminosilicate by inner–sphere complexes formation is enhanced when dissolved CO_2 species exist in the system. It is reported that sulfate modifies the surface charge of aluminum hydroxide gels by inner–sphere complex formation, and produces negative charges that enhance the cation adsorption capacity of the gels (Micera 1984). This supports the mechanism of the dissolved CO_2 effect which I proposed above.

The effect of dissolved CO_2 on Zn adsorption onto amorphous aluminosilicate can be seen most specifically at around 100 μmol / L (Fig. 5–6). This concentration of Zn corresponds to 6.5 ppm. On the other hand, the concentration of HCO_3^- in the experiment is calculated to be equilibrated with 23000ppm of soil air CO_2. The reported values of Zn concentration in natural water and the maximum concentration of CO_2 in soil air are listed in Table 5–3 and 5–4, respectively. From the tables it can be seen that the experimental condition, both 100 μmol / L of Zn and 2 mmol / L of HCO_3^-, are available in natural system. Therefore, the effect of dissolved CO_2, which increases the adsorption amount of Zn onto amorphous aluminosilicate would be observed in nature. The results of laboratory experiments suggested the possibility that the seasonal

Table 5-3 Reported concentration of Zn in natural water.

Zn (ppm)		
4 ~ 270	(Kabata and Pendias 1984)	
7137	very acidic soil pH < 4	(Kiekens 1981)
10 ~ 30	slightly acidic lake	(Sigg 1995)
~ 0.9	natural water	(Yamagata 1980)
~ 16	un-polluted stream water	(Runnels et al. 1994)
25	stream water near a mine	(Runnels et al. 1994)

Table 5-4 Reported maximum concentration of CO_2 in soil air.

CO_2 (μL/L)		
15000	New Zealand forest	Gunn and Trudgill (1982)
12500	New England spruce and fir forest	Fernandez and Kosian (1987)
14000	Virginia desiduous forest	Castelle and Galloway (1990)
8000	French rendzina (upper 25cm)	Durand (1980)
8000	forested Siberian chernozem	Vugakov and Popova (1968)
70000	cultivated soil	Buyanovsky and Wagner (1983)

variation of the CO_2 concentration in soil air could be a factor in controlling the heavy metal concentration of soil water.

In conclusion, the laboratory experiments were performed using HCO_3^- to examine if CO_2 partial pressure in soil air can affect the solid–liquid interfacial reaction between Zn ions and amorphous aluminosilicate. The results obtained suggest that the amount of adsorbed Zn onto the solid is increased by existence of HCO_3^-. The assumed mechanism of this reaction by XANES spectra is modification of the solid surface by inner–sphere complexation of HCO_3^-, which enhance adsorption of Zn ions. These results suggest the necessity to take the components of soil air into account when dealing with solid–liquid interfacial reactions of heavy metal ions in soil systems.

(2) Natural Sample Analysis

The laboratory experiments suggested the possibility that the seasonal variation of CO_2 concentration in soil air can cause seasonal variation of soil water composition. Since there are no data about seasonal variation of heavy metal concentration in soil water concerning CO_2 partial pressure in soil air, I constructed a new system by which one can obtain soil water and the CO_2 composition of soil air at same time. The system was tested in Miho forest in Yokohama. It is a wooded suburban area composed mainly of deciduous trees.

Miho forest has many springs. I selected a slope faces to a spring, because at there I can collect soil water together with spring water and it is possible to compare the composition of soil water with spring water. The most important thing in the soil water sampling is to choose a place whose underground is rich in water, otherwise it is impossible to collect enough amount of soil water. When the point which I selected was not rich in water and it was impossible to collect soil water, I had to change the sampling point to another place. Finally, I selected a point which is 50 cm from a deciduous tree on the slope. The color of the soil is dark brown from the surface to the depth of 30cm. This color of the soil seems to indicate high contents of organic substance. Deeper than 30 cm, the color of the soil changes to light brown. This soil is fine and can be supposed to be rich in clay materials.

Table 5–5 shows observed seasonal variation of CO_2 concentration in soil air. It can be seen that the concentration of CO_2 increased form April to August and decreased in September. The observed seasonal variation is consistent with previous reports by Fernandez and Kosian (1987). In Table 5–5 however, the maximum concentration of CO_2, 2400 ppm, seems to be lower compared with the reported values of maximum CO_2 concentrations in soil air which are listed in Table 5–4. I think this difference is due to the difference of soil structure. The soil in Miho forest is supposed to have porous structure and the soil air can

Table 5–5. Concentration of CO_2 in soil air.

Date	Temperature	CO_2 concentration in soil air (ppm)				
	(℃)	10cm	20cm	30cm	40cm	50cm
1994. 4.29	19.9	360	550	480	550	460
6. 4	24.6	500	700	800	850	700
7. 6	30.1	800	900	1050	1100	1000
1995. 4.12	10.8	360	600	600	750	900
7. 4	21.9	—	—	—	2400	1900
8. 3	26.6	1200	1000	1700	2100	2400
10.24	15.3	700	1200	1500	1600	2000

– means that the data could not obtained.

mix easily with the atmosphere. Castelle and Galloway (1990) reported that there is a strong correlation between soil temperature and CO_2 concentration in soil air, while soil moisture content is weakly related with CO_2 concentration in soil air. However, in Moho forest I think the soil water easily evaporate because of the porous structure of the soil and this will promote the soil gas to mix with the atmosphere.

The depth profile of CO_2 concentration in soil air is shown in Table 5–5. In the depth profile 40 or 50 cm has maximum CO_2 concentration. This is completely consistent with the results obtained by Castelle and Galloway (1990). At the depth of 40 and 50 cm, it was observed that the soil had different color from the upper part and the lower part of the soil seemed to have more packed structure. I think the packed soil structure, which obstructs the soil air to mix with the atmosphere, is the main reason for the obtained depth profile (Table 5–5).

One may notice that the CO_2 concentration in soil air is higher in 1995 than in 1994 (Table 5–5). This is mainly due to an improvement of the sampling system. For the soil gas sampling, the most important thing is to make the sampling system completely air tight. In 1995, the system was improved a bit and it was made air tight as much as possible.

Table 5–6 shows the data on concentrations of dissolved CO_2. There is few method which is effective to analyze the amount of dissolved carbon diox–

Table 5–6 Concentration of dissolved CO_2 in soil water.

Depth (cm)	pCO_2 (ppm)	pH	Dissolved CO_2 (mmol/L)	*Equilibrated CO_2 (ppm)
10	360	–	–	–
20	550	–	–	–
30	480	–	–	–
40	550	–	–	–
50	460	–	0.59	2700
spring water		6.96	0.68	4800

* Calculated concentration of CO_2 equilibrated with disslbed CO_2
Sampling was performed on 1994.4.27

– means data could not obtained.

ide. Although a general method is alkaline titration, end point of the titration is unclear in this method. Therefore, I used trace diffusion method (Oana 1954). In this method, a known amount of sample is mixed with H_2SO_4 to release dissolved CO_2 species as CO_2 gas in a closed container. The released CO_2 is adsorbed by known amount of $Ba(OH)_2$ aquatic solution, then the amount of alkaline which did not react with released CO_2 is titrated by HCl aquatic solution.

In Table 5–6, the concentration of dissolved CO_2 is shown with calculated concentration of CO_2 in the soil air which is equilibrated with the observed dissolved CO_2. It can be seen the measured CO_2 concentration in soil air is much lower than the equilibrium CO_2 concentration calculated by using the measured concentration of dissolved CO_2. The reason for this difference is still unclear. However, I think it is possible that organic carbon dissolved in the collected soil water, for example humic acid, was oxidized by H_2SO_4 and released CO_2 gas. Therefore, in the future it will be necessary to adopt more suitable analytical method to measure the concentration of dissolved inorganic CO_2 species. Recently, an experimental method to analyze dissolved CO_2 by ion chromatography was developed (Hayakawa *et al.* 1993). It will be necessary to apply such analytical method to analyze only the dissolved inorganic CO_2 species in soil water selectively.

In Table 5–6, the concentration of dissolved CO_2 in soil water is almost

half of the concentration in spring water. The dissolved CO_2 concentration in spring water is equilibrated with the soil air from where the water obtained CO_2 (Yoshimura and Inokura 1985). Therefore, it is supposed that the spring water reacted with soil air which had higher value of CO_2 concentration than the soil air at 50 cm.

Table 5-7 shows obtained Zn concentration in soil water. There can be seen some difference between depths and seasons. Since the differences are more than the error, it can be said that Zn concentration in soil water has variety depending on depth and season. The concentration of Zn at 10 cm of depth is much lower than the obtained values at lower place. I think this is due to Zn adsorption onto organic substances which is supposed to be rich in the surface part of soil. The Zn concentration in soil water collected in April 1994 at 50 cm is higher than that of 40 cm. This also can be explained by the supposed decrease in contents of organic substance in lower part of the soil.

When we compare the concentration of Zn in soil water at the depth of 50 cm, the concentration in April 1994 is higher than that of August 1995. The results of laboratory experiments suggested that when the concentration of CO_2 partial pressure in soil air is high, the amount of Zn adsorbed onto solid will be increased. Therefore, it is supposed that Zn concentration in soil water would be low in summer when the partial pressure of CO_2 is high and adsorption of Zn onto solid is promoted. On the other hand, Zn concentration in soil water is

Table 5-7 Zn concentration in soil water.

Sample		Concentration of Zn (ppm)
1994. 4. 27	40cm	0. 187
	50cm	0. 262
1995. 4. 12	10cm	0. 0034
8. 3	50cm	0. 0267

supposed to be high in winter. Although the observed concentration of Zn in soil water and the maximum partial pressure of CO_2 are lower than the experimental condition, the observed result (Table 5–7) is not inconsistent with the results of laboratory experiment.

The above is the data obtained by the system tested at Miho forest. I could analyze Zn concentration in soil water and the concentration of CO_2 in co–existing soil air by using the sampling system. This system can be concluded to be effective in monitoring the compositions of soil water and soil air. From now on, it will be necessary to collect sampling data for years. On the way, analytical procedures will have to be improved.

5–4 CONCLUSION

The effects of soil air composition on the solid–liquid interfacial reactions of heavy metal ions were examined. In batch adsorption experiments, a $NaHCO_3$ aquatic solution was used to simulate the variation of CO_2 concentration in soil air.

By the experiments, it was clarified that the CO_2 concentration in soil air affects the solid–liquid interfacial reaction between Zn ions and amorphous aluminosilicate. The co–existing HCO_3^- enhances Zn adsorption, in the range concentrations of Zn and dissolved CO_2 lower than the solubility product of $ZnCO_3$. The mechanism of this reaction is assumed to be modification of the amorphous aluminosilicate surface by an inner–sphere complex formation of HCO_3^-, which increases the affinity of the surface for Zn ions.

The results obtained by laboratory experiments suggested the necessity of taking the composition of soil air into account when dealing with solid–liquid interfacial reactions of heavy metal ions in soil systems. To observe the relationships between the composition of soil air and water, a new system was constructed, and tested in a wooded suburban area. It was possible to obtain data on the Zn concentration in soil water and the CO_2 concentration in soil air. The relationship observed between the seasonal variation of Zn concentration in the soil water and CO_2 partial pressure in the soil air was consistent with the results of laboratory experiments.

REFERENCE

Anderson, J.P.E. (1982) 41. Soil respiration. in *Methods of soil analysis, part 2. Chemical and microbiological properties*. S. Segoe Rd., Madison, USA.

Bolt, G.H. and Bruggenwert M.G.M (1989) 1. Component of soil. in *Soil Science*. (eds.) Bolt G.H. and Bruggenwert M.G.M., gakujyutu syuppann center, Tokyo.

David, M.B. and Vance, G.F. (1989) Generation of soil solution acid–neutralizing capacity by addition of dissolved inorganic carbon. *Environ. Sci. Technol.*, **23**, 1021–1024.

Fernandez, I.J. and Kosian, P.A. (1987) Soil air carbon dioxide concentrations in a New England spruce–fir forest. *Soil Sci. Soc. Am. J.*, **51**, 261–263.

Hayakawa, K. *et al.*, (1993) Ion chromatographic Determination of Carbonate–Carbon. *Bunseki*, **5**, 375–378.

Jenkinson, D.S., Adams, D.E. and Wild, A. (1991) Model estimates of CO_2 emissions from soil in response to global warming. *Nature*, **351**, 304–306.

Micera, G *et al.*, (1984) Anion–induced metal binding in amorphous aluminum hydroxide. *Colloid and Surface*, **11**, 109–117.

Minami, K. (1991) Emission of biogenic gas compounds from soil ecosystem and their effects on global environment. 1. General remarks. *Nihon Dojyou Hryougaku Zasshi*, **62**, 445–450.

Oana, S., (1954) Analytical method for dissolved gases in water. *Japan Analyst*, **3**, 522–528.

Ouyang, Y. and Boersma, L. (1992) Dynamic oxygen and carbon dioxide exchange between soil and atmosphere: 1. Model development. *Soil Sci. Soc. Am. J.* **56**, 1695–1702.

Russ J.O. and Johnson D.W. (1985) Effect of soil process on the acidification of water by acid deposition. *J. Environ. Qual.*, **14**, 26–31.

Stumm, W. and Morgan, J.J. (1981) 4. Dissolved carbon dioxide. in *Aquatic chemistry*. 2nd ed. A Willy–interscience publication, New York.

Tsuruta, H. (1992) Emission of biogenic gas compounds from soil ecosystem and their effects on global environment. 5. Carbon dioxide. *Nihon dojyo hiryougaku zassi*, **63**, 237–244.

Tsuruta, H. (1994) 2. Carbon dioxide. in *Soil and Atmosphere* (ed.) Minami. K. Asakura syoten, Tokyo.

Yoshimura K. and Inokura Y. (1985) Chemical components and variation of their contents of groundwaters in the southern area of Akiyoshi–dai (Plateau).

CHAPTER 6: CONCLUSION

In this thesis, I studied the interaction between heavy metal ions and soil particles in solid–liquid interfacial reactions. In each chapter, I examined the solid–liquid interfacial reactions from different angles using amorphous aluminosilicate as a model substance for the surface of soil particles. The results which I obtained and described in each chapter are outlined below.

In Chapter 2, I synthesized the model substance by the co–precipitation method. The precipitate obtained was characterized as allophane–like amorphous aluminosilicate. The allophane–like amorphous aluminosilicate was concluded to be suitable as a model substance for the surface of soil particles in dealing with the solid–liquid interfacial reaction of heavy metal ions. Therefore, in the following chapters, this aluminosilicate was used as the solid phase.

In Chapter 3, the quantitative aspects of solid–liquid interfacial reactions between the amorphous aluminosilicate and zinc ions were clarified. Here I developed a new batch adsorption method so as to maintain constant the ionic strength and the pH value of the reacting suspension and vary only the concentration of heavy metal ions. The new method was helpful in discussing solid–liquid interfacial reactions quantitatively. Using this method, I could obtain the following results.

Zinc ions react differently with two types of surface hydroxyl groups, i.e., aluminol and silanol. At the silanol sites, zinc ions precipitate as $Zn(OH)_2$. On the other hand, zinc ions form an inner–sphere complex at the aluminol site. The precipitation is formed slowly, while the surface complex formation reaches an equilibrium within 30 minutes. Therefore, one may surmise that in natural soil systems the former reaction is regulated by the reaction rate and the latter reaction is controlled by equilibrium constants.

It was determined that the surface complex is formed between one Zn^{2+} ion and two aluminol groups. However, when the concentrations of both solid and zinc ions in a suspension were low, a surface complex between a monovalent Zn–complex ion such as $Zn(NO_3)^+$ and an aluminol group was found.

In Chapter 4, spectroscopic approaches were made to the solid–liquid interfacial reactions. Using Mössbauer spectroscopy and XAFS (X–ray Absorption Fine Structure), the chemical states of zinc, ferrous and ferric ions could be determined on the wet surface of amorphous aluminosilicate.

On the amorphous aluminosilicate, zinc ions were found to form an inner–sphere complex with aluminol groups. This finding is consistent with the results noted in Chapter 3. The surface complex of zinc was found to have a local structure similar to a tetrahedral unit in $Zn(OH)_2$.

Ferrous ion was found to form an outer-sphere complex on the surface of amorphous aluminosilicate. On the other hand, ferric ion was found to form an inner-sphere complex, in which the chemical state of the ion is similar to that of a ferric ion which has replaced the aluminum in the six-coordinated site of allophane.

In Chapter 5, the effects of co-existing chemical species on solid-liquid interfacial reactions were examined. Here, the hydrogencarbonate ion was adopted especially in order to discover the effects of CO_2 concentration in soil air. By adsorption experiments using the batch method developed in Chapter 3, it was found that the amount of zinc adsorbed onto amorphous aluminosilicate increases when HCO_3^- exists in the suspension. This finding indicated the possibility that the seasonal variation of CO_2 partial pressure in the soil air can affect heavy metal movement in soil systems and the composition of soil water.

In this thesis, Chapters 3, 4, and 5 correspond respectively to quantitative analysis, state analysis and examination of the effect of co-existing substances. These are the three main steps when we clarify the mechanisms of chemical reactions. In this study, the mechanisms of zinc, ferrous and ferric ion adsorption onto amorphous aluminosilicate could be described as chemical reactions: inner-sphere complex formation, outer-sphere complex formation or precipitation on the surface. Therefore, the purpose of this study, to detail the solid-liquid interfacial reactions of heavy metals in soil systems as chemical reactions, was accomplished in the case of amorphous aluminosilicate and zinc, ferrous, and ferric ions.

The findings of this study can be developed in two directions in the future. One is to clarify the details of solid-liquid interfacial reactions on soil particles. For this, the batch adsorption method which was developed in this study and spectroscopic analysis will be helpful. The other direction is to analysis the heavy metal movement in natural systems by the mechanisms obtained. For this purpose, the system I constructed in Chapter 5 to monitor soil water composition and CO_2 concentration in soil gas is certain to be useful.

Soil is a very complex system; however, its importance demands that we understand this complexity. Since phenomena in soil systems are the result of many chemical reactions, it is necessary to understand chemical reactions in soil systems. I hope that this study will be developed further in the quest to understand soil, the basis of our life.

ACKNOWLEDGEMENTS

I would like to thank Prof. Motoyuki Matsuo with all my heart for his support as supervisor throughout my years in the doctoral course.

I also wish to thank Prof. Bokuichiro Takano for his helpful comments on my work. Thanks are likewise extended to Dr. Katsuhiko Suzuki.

Prof. Takuji Yokoyama of Kyushu University gave me many useful suggestions regarding my work and much encouragement. Prof. Izumi Nakai provided valuable mechanical support for the XAFS measurements at the Photon Factory in Tsukuba. Prof. Haruo Sato gave me detailed information about the preparation of $FeCl_2$. Mr. Jeffrey Clark made helpful correction in the phrasing of this thesis.

I would like to extend heartfelt thanks to all of them as well as to the laboratory members and my family who gave me their support.

BIBLIOGRAPHY

1. Miyazaki, A. and Tsurumi, M. (1995) The H^+/Zn^{2+} exchange stoichiometry of surface complex formation on synthetic amorphous aluminosilicate. *Journal of Colloid and Interface Science*, **172**, 331-334.

2. Miyazaki, A., Matsuo, M. and Tsurumi, M. Surface complex formation between Zn ion and amorphous aluminosilicate in aquatic systems. *Journal of Colloid and Interface Science*, **177**, 335-338.

3. Miyazaki, A. and Matsuo, M. A study on adsorption states of ferrous and ferric ions on amorphous aluminosilicate. *Il Nuovo Cimento D* (conference proceedings of ICAME-95), in press.